J Membrane Biol (2014) 247:211–229
DOI 10.1007/s00232-013-9626-8

Long Open Amphotericin Channels Revealed in Cholesterol-Containing Phospholipid Membranes Are Blocked by Thiazole Derivative

Oleg Ya. Shatursky · Olexander V. Romanenko · Nina H. Himmelreich

Received: 26 August 2013 / Accepted: 26 December 2013 / Published online: 9 January 2014

Abstract The action of antifungal drug, amphotericin B (AmB), on solvent-containing planar lipid bilayers made of sterols (cholesterol, ergosterol) and synthetic C14–C18 tail phospholipids (PCs) or egg PC has been investigated in a voltage-clamp mode. Within the range of PCs tested, a similar increase was achieved in the lifetime of one-sided AmB channels in cholesterol- and ergosterol-containing membranes with the C16 tail PC, DPhPC at sterol/DPhPC molar ratio $\leq$1. The AmB channel lifetimes decreased only at sterol/DPhPC molar ratio >1 that occurred with sterol/PC molar ratio of target cell membranes at a pathological state. These data obtained on bilayer membranes two times thicker than one-sided AmB channel length are consistent with the accepted AmB pore-forming mechanism, which is associated with membrane thinning around AmB–sterol complex in the lipid rafts. Our results show that AmB can create cytotoxic (long open) channels in cholesterol membrane with C14–C16 tail PCs and nontoxic (short open) channels with C17–C18 tail PCs as the lifetime of one-sided AmB channel depends on $\sim$2–5 Å difference in the thickness of sterol-containing C16 and C18 tail PC membranes. The reduction in toxic AmB channels efficacy can be required at the drug administration because C16 tails in native membrane PCs occur almost as often as C18 tails. The comparative analysis of AmB channel blocking by tetraethylammonium chloride, tetramethylammonium chloride and thiazole derivative of vitamin B_1, 3-decyloxycarbonylmethyl-4-methyl-5-(2-hydroxyethyl) thiazole chloride (DMHT), has proved that DMHT is a comparable substitute for both tetraalkylammonia that exhibits a much higher affinity.

Keywords Amphotericin B · Membrane thinning · Lipid bilayers · DMHT compound

O. Ya. Shatursky (✉) · N. H. Himmelreich
Department of Neurochemistry, Palladin Institute of Biochemistry, Leontovich Str., 9, Kiev 01601, Ukraine
e-mail: olegshatursky@biochem.kiev.ua

O. V. Romanenko
Department of Biology, Bogomolets National Medical University, Pobedy Av., 34, Kiev 03680, Ukraine

Introduction

Amphotericin B (AmB) is a polyene antibiotic that is cytotoxic for many fungal infections and one of the few available fungicidal drugs. Despite significant achievements in lipid-associated drug delivery formulations that drastically reduced AmB toxicity for the patients, AmB can still cause decreased renal function, anorexia, high fever, nausea, memory difficulties, confusion and other side effects (Hartsel and Bolard 1996; Glasser and Murray 2011). Most of the classic and contemporary research tends to explain the mechanism of AmB cytotoxicity by its concentration-dependent pore formation in the target cell plasma membrane (Marty and Finkelstein 1975; Maeng et al. 2010). This type of AmB action is thought to be responsible for affected cell swelling, cellular homeostatic responses and apoptotic effects (Yano et al. 2009). The preferential activity of AmB on ergosterol-containing membranes versus cholesterol-containing membranes endows it with its antifungal activities (Cohen 2010) and led researchers to a preferential use of ergosterol-containing model membranes to explore the AmB mode of action (Bolard et al. 1991; Brutyan and McPhie 1996).

The generally accepted AmB mode of action is that the formation of intermolecular hydrogen bonds between AmB monomers stabilizes a complex of eight to ten AmB monomers (Marty and Finkelstein 1975; Baginski et al.

1997), which either partitions or penetrates into the lipid bilayer on one side of membrane (Bolard et al. 1991; Romero et al. 2009; Lisnyak 2012). Two types of resulting "nonaqueous" and "aqueous" AmB channels (the latter also referenced as one-sided channel or water pore (Marty and Finkelstein 1975; Brutyan and McPhie 1996; Romero et al. 2009) are cation-selective. Another type of AmB channel is a symmetrical or double-channel (Marty and Finkelstein 1975; Ostroumova et al. 2012) that is composed of two cation-selective channels formed on the opposite sides of membrane and bound into a single, membrane-spanning ion-conducting complex. The double-channel model preferentially passes anions and is unlikely to contribute to AmB-induced cytotoxicity (Marty and Finkelstein 1975; Brutyan and McPhie 1996; Ostroumova et al. 2012). Thus, the thickness of lipid bilayer determines whether a toxic or nontoxic AmB water pore is formed.

Previous studies have suggested that AmB and nystatin cation-selective channels can be formed on solvent-containing membranes (also known as "painted" bilayers; Marty and Finkelstein 1975; Mueller et al. 1962), but because the length of AmB molecule (28 Å) is less than thinnest solvent-containing bilayer (~30 Å; Montal and Mueller 1972; Gross et al. 2011), the use of solvent-free (thin) bilayer lipid membranes (BLMs) has been favored for studies of one-sided AmB channel conductance (Marty and Finkelstein 1975; Brutyan and McPhie 1996; Venegas et al. 2003). The latest advances in understanding of AmB pore formation suggest that AmB water pores reduce the membrane thickness by locally removing cholesterol molecules from interaction with phospholipid molecules, which results in the formation of AmB–cholesterol complexes (Cohen 2010). This observation provided support for the idea that membrane lipids are compressed around AmB water pore weakened by alternative suggestion that cholesterol does not potentiate one-sided action of AmB (Marty and Finkelstein 1975; Bolard et al. 1991), thus making the overall membrane thickness a major limitation for stable AmB channel creation. The fact that the depth of membrane hydrocarbon core around AmB–cholesterol complex is compatible with its length suggested the use of thick solvent-containing bilayers formed from cholesterol and short-chain phospholipids to investigate AmB channel conductance. The observations of one-sided AmB action on thin cholesterol-containing phospholipid bilayers failed to find the long dwelling channels (Brutyan and McPhie 1996) or any channels at all (Bolard et al. 1991), suggesting that AmB cytotoxicity on mammalian cells is not achieved by water pore formation. There are, however, studies that show Na^+ influx via the formation of cholesterol-dependent AmB water pores in kidney tubular cells is responsible for the increase in cytosolic Ca^{2+} concentration (Yano et al. 2009), which may cause cell death (Cohen 2010; Bernardi and Rasola 2007). Besides the increase in cholesterol and sphingomyelin concentration around one-sided AmB water pores, formed in kidney cells plasma membrane, AmB channels are also linked to an increase in ceramide, known to be a second messenger in activating the apoptotic cascade (Zager 2000). These data provide more grounds to doubt common suggestion that greater affinity of AmB for ergosterol-containing membranes of fungi versus cholesterol-rich mammalian cell membranes excludes most of harm that could be done to AmB-treated patients. Conversely, the acute and chronic toxicity towards humans provides ample evidence that AmB selectivity to ergosterol-containing fungi cells is not absolute even within novel drug delivery formulations (Hartsel and Bolard 1996; Glasser and Murray 2011).

This paper represents the comparative analysis of AmB action we explored on thick "painted" cholesterol- and ergosterol-containing BLMs formed from egg phosphatidylcholine (PC) and synthetic phospholipids with tail lengths ranging from 14 to 18 carbons. The results support the concept of toxic/nontoxic one-sided AmB channel formation that takes place due to different mechanisms of target cell membrane thinning determined by the difference in length between 16 carbon tails and 18 carbon tails of plasma membrane phospholipid at the boundary of raft and nonraft bilayer where the membrane thickness is greater than that of nonraft bilayers (Cohen 2010). The possibility that the long open states exhibited by one-sided AmB channel in "painted" cholesterol-containing 16 carbons tail phospholipid planar bilayer membrane cause persisting drug toxicity within 16 carbon tails phospholipid environment of mammalian cell plasma membrane is discussed. The application of thiazole derivative, DMHT, as a novel high-affinity blocker of AmB channels that has already proved its efficacy on cytotoxic and neurotoxic pore-forming proteins (Romanenko et al. 1995; Shatursky et al. 2007) was proposed to reduce polyene antibiotics toxicity and improve its less efficient test systems developed on thin cholesterol-containing lipid bilayers (Brutyan and McPhie 1996).

Materials and Methods

Amphotericin B, metal chlorides (potassium, calcium, lithium, cesium), *n*-heptane, ergosterol, Tris–HCl, dimethyl sulfoxide (DMSO), tetramethylammonium chloride (TMA), tetraethylammonium chloride (TEA), glycerol and polyethylene glycols (PEGs) were purchased from Sigma-Aldrich Chemie GmbH (Steinheim, Germany). The planar bilayers were formed by Mueller et al. (1962) from *n*-heptane solution of cholesterol (Avanti Polar Lipids, Alabaster, AL, USA) or ergosterol and phospholipids: egg

phosphotidilcholine (egg PC; Kharkov factory of biopreparations Biolek, Ukraine), 1,2-dimyristoyl-*sn*-glycero-3-phosphocholine (DMPC), 1,2-dipentadecanoyl-*sn*-glycero-3-phosphocholine, 1,2-diphytanoyl-*sn*-glycero-3-phosphocholine (DPhPC), 1,2-diheptadecanoyl-*sn*-glycero-3-phosphocholine, 1,2-distearoyl-*sn*-glycero-3-phosphocholine (DSPC) and 1,2-dioleoyl-*sn*-glycero-3-phosphocholine (DOPC) (Avanti Polar Lipids, Alabaster, AL, USA). The mixtures of cholesterol/phospholipids and ergosterol/phospholipids were usually kept at a weight ratio of 1/2. The sterol/DPhPC weight ratios of 1/1; 0.5/2.5; 2/1 equivalent to the cholesterol/DPhPC molar ratios of 2.59/1.18; 1.3/2.95; 5.18/1.18 and ergosterol/DPhPC molar ratios of 2.52/1.18; 1.26/2.95 correspondingly were used in a separate set of experiments to define the dependence of ionic channels lifetime and insertion rate on the concentration of membrane sterols. The total lipid concentration in heptane solution was 20 mg/ml. Several times spread and dried membrane solution was used to pretreat the aperture before the membrane formation. Lipid bilayer membranes were painted across a round aperture (0.5 mm diameter) in a thinned wall of a Teflon cup held within a glass chamber. The blackening of bilayer membrane was monitored visually with an MBS-9 binocular microscope (St. Petersburg Optico–Mechanical Plant LOMO, Russian Federation) in reflected light. The membrane was illuminated via a light guide. The inner volume of Teflon cup was 1 ml, whereas the outer glass compartment contained 9 ml of the membrane bathing solution. The membrane separated solution contained 10 mM Tris–HCl (pH 7.4) and the required quantities of analytical grade salts: potassium chloride, sodium chloride (USB, Cleveland, OH, USA), calcium chloride, lithium chloride and cesium chloride. The buffered solutions in both chambers could be stirred as required.

Amphotericin B powder was dissolved to 2 mM in DMSO and diluted with the same saline of membrane bathing solution. Stock solution was kept at a room temperature in the dark for $\sim$4 h time and then discarded. The final concentration of DMSO in the chamber usually was 10^{-3} % on either side of BLM. In control experiments, DMSO at the concentrations $<10^{-1}$ % never affected the conductance of painted cholesterol- and ergosterol-containing phospholipid membranes.

Voltage-clamp recordings of transmembrane current were made via a high-resolution home-made amplifier with 0.1-kHz bandwidth. The chamber inside Teflon cup was referred as the *trans*-side of membrane, which was defined as a virtual zero. The outer glass compartment was referred to as the *cis*-side. Both *cis*- and *trans*-chambers were connected with amplifier through a pair of agar bridges immersed into a 2-M KCl solution with silver chloride electrodes. The polarization potential between assembled electrodes did not exceed 1.5 mV. The voltage source enabled us to apply voltage-ramp protocols of 60 mV/min or holding potentials within the range of $\pm$100 mV. Transmembrane currents were recorded on an N307/1 XY recorder (ZIP, Krasnodar, Russian Federation). Semi-conductor thermobatteries TEMO-3 (Lvov Factory Electronpribormash, Ukraine) were used to apply a temperature ramp or steady temperatures within the range of 4–40 °C. The stirring of the membrane bathing solutions minimized the error of uneven warming or cooling. Activation energy of AmB-modified cholesterol–DPhPC BLM bathed in the solution containing 100 mM KCl was defined as in Shatursky et al. (2007).

Tetraalkylammonia, TMA and TEA were used as standard blockers of AmB channels. Thiazole derivative of vitamin B_1, 3-decyloxycarbonylmethyl-4-methyl-5-(2-hydroxyethyl) thiazole chloride (DMHT):

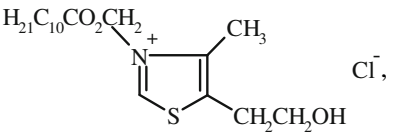

was synthesized by Dr. A.I. Vovk of the Institute of Bioorganic Chemistry and Petroleum Chemistry (Kiev, Ukraine) as described in Romanenko et al. (1995). In all conductance blocking experiments, TMA, TEA and DMHT were dissolved with the same saline as in BLM bath.

The radii of pores formed by AmB channels were defined by the method of Krasilnikov et al. (1998). Low molecular weight nonelectrolytes of analytical grade, including ethylene glycol (Riedel-de-Haen, Seelze, Germany), glycerol, glucose (Fluka Chemie GmbH, Buchs, Switzerland), sucrose (Fluka Chemie GmbH, Buchs, Switzerland) and polyethylene glycols (PEGs) with average molecular weight of 300 and 400, were mixed with the basic membrane bathing solution of 2 M KCl (pH 7.4) at a final concentration of 20 %. Total conductivity of the solutions was measured by Radelkis OK 102/1 conductivity meter (Budapest, Hungary).

The capacitance of cholesterol–DPhPC and cholesterol–PC BLMs was measured by application of triangular voltage to obtain a square wave capacitive current output (Gross et al. 2011). A triangular wave with 50-mV positive peak amplitude and 100-ms period was applied to a lipid bilayer with a diameter of 252–280 μm for less than 1-min time. Total BLM capacitance (C_T) was calculated from the resulting capacitive current (I_C) by the equation: $I_C = C_T \times dV/dt$. A calibrated capacitor of 235 pF was used to determine dV/dt. Specific BLM capacitance (C) was determined by following equation: $C = \varepsilon\varepsilon_0 C_T/d$, where ε is the dielectric constant of membrane hydrocarbon region, ε_0 is the dielectric permittivity of vacuum (8.85×10^{-12} F/m),

and d is a thickness of BLM. All experiments were carried out at room temperature (20–24 °C), unless otherwise stated. Hereinafter, mean values ± standard deviations are indicated for 10–20 experiments, each made on a freshly painted bilayer membrane. Statistical calculations were made by Origin Pro 8.6.0 software.

Results

Reconstitution of AmB Channels from One and Two Sides of Solvent-Containing Membrane

Addition of AmB into the solution with 2 M KCl on the *cis*-side of cholesterol–C16 acyl chain phospholipid (DPhPC) membrane at a final concentration more common for nonaqueous pore formation 0.02 μg/ml (Legrand et al. 1997) caused ~100-fold increase in conductance that resulted in appearance of steady-state macroscopic current. Similar results were obtained after the addition of the same AmB concentration to the *cis*-side of cholesterol–C14 (DMPC) or C15 (1,2-dipentadecanoyl-*sn*-glycero-3-phosphocholine) acyl chains phospholipid membranes. The macroscopic conductance of cholesterol–egg PC (C16, C18 acyl chains) BLM steadily increased only after AmB application into near membrane area. This type of introduction caused an increase in current almost instantly as the AmB concentration consisted of 0.03–0.07 μg/ml near membrane washed in the solution with 100 mM KCl or 2 M KCl (data not shown). The membrane conductance rose five–10-fold to a peak and than decayed over 10–15-min time to zero level reappearing again in form of relatively short sudden bursts of simultaneous multiple-channel activities lasting tens of seconds at best. The instable growth of macroscopic current resulting from short (lasting seconds and less) single- and multiple-channel openings was also produced by the addition of AmB into the solution of 2 M KCl on the *cis*-side of cholesterol–egg PC membrane away from near membrane area. Conversely, the increase in transmembrane current achieved on cholesterol-containing C14, C15 or C16 tail phospholipid [DMPC; 1,2-dipentadecanoyl-*sn*-glycero-3-phosphocholine; DPhPC (each tested separately)] membranes either eventually reached a steady state or was stopped by washout with antibiotic-free saline and also remained stable. This suggests that one-sided AmB channel retains its long open states that last minutes and more in cholesterol-containing membranes with C14–C16 tail phospholipids listed.

Above observations are in agreement with the results on one-sided insertion of AmB and nystatin channels into thin cholesterol–phospholipid BLM (Marty and Finkelstein 1975; Bolard et al. 1991). Previous research has also proven much smaller AmB threshold concentrations (≥0.036 μg/ml) required for water pore formation in thin cholesterol–DPhPC planar bilayers (Brutyan and McPhie 1996) as compared with those reported for

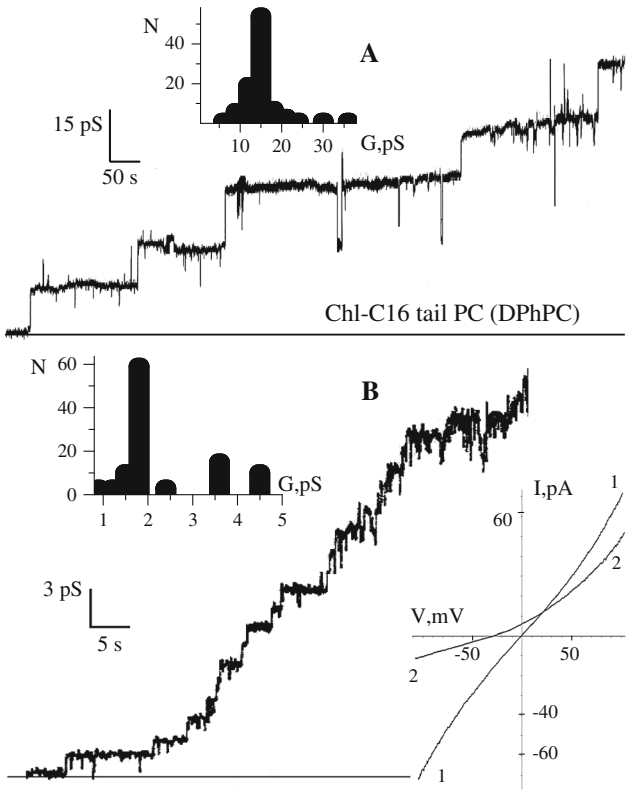

Fig. 1 Single channels created after the separate addition of AmB from the *cis*-side and consecutive addition of AmB from the *cis*- and the *trans*-sides of planar bilayer membrane at a potential of 115 mV. **a** (Chl-C16 tail PC) AmB was added to the *cis*-chamber with cholesterol–DPhPC membrane (molar ratio of 2.59/2.36) at a final concentration of 0.005 μg/ml. The membrane washing solution contained 2 M KCl, 10 mM Tris–HCl (pH 7.4). The single channels record was obtained after continuous monitoring of transmembrane current for 15–20 min. Channel openings are shown as upward deflections. *Solid line* represents zero current. Amplitude histogram of one-sided AmB channel conductance was defined under above conditions. **b** AmB was present from the *cis*- and *trans*-side of cholesterol–egg PC membrane at a concentration of 0.0005 μg/ml. The cholesterol–egg PC molar ratio of the membrane was 2.59/2.60. The membrane washing solution contained 2 M KCl, 10 mM Tris–HCl (pH 7.4). Single channels were recorded after continuous monitoring for 15–20 min time. Channel openings are shown as *upward* deflections. *Solid line* represents zero current. Amplitude histogram of AmB double-channel conductance defined under above conditions on ~100 single-channel events is shown in the *left* side. The *I/V* plots on the *right* side represent steady-state current–voltage relationships of cholesterol–egg PC membrane (the molar ratio of 2.59/2.60) modified with AmB double-channels. The membrane separated solution contained: *curve 1*—2 M KCl, 10 mM Tris–HCl (pH 7.4) from both sides of the membrane; *curve 2*—0.2 M KCl, 10 mM Tris–HCl (pH 7.4) from the *cis*-side and 2 M KCl, 10 mM Tris–HCl (pH 7.4) from the *trans*-side of membrane. In cases **a** and **b,** the surface of actual bilayer membrane formed on 0.5-mm-diameter hole in Teflon cup was $\sim 0.55 \times 10^{-4}$ cm^2

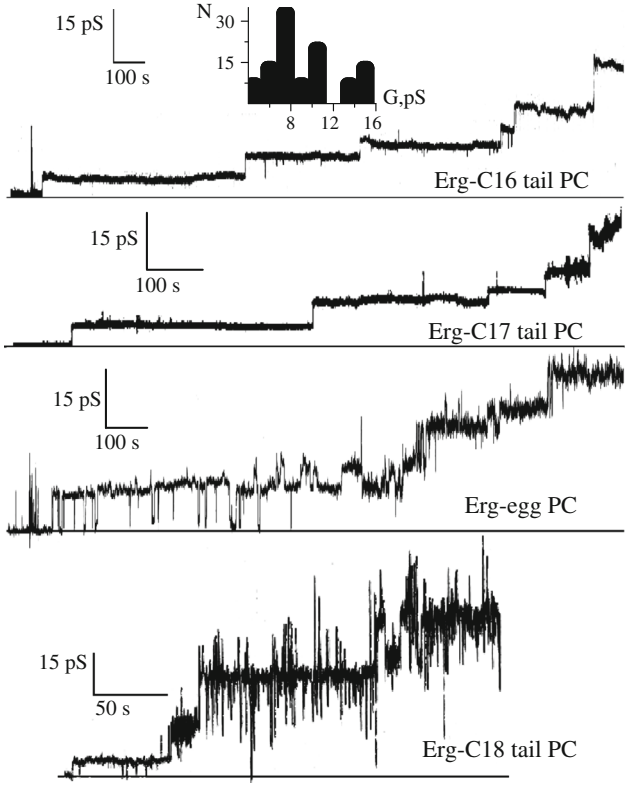

Fig. 2 Single channels created after the addition of AmB from the *cis*-side of ergosterol-containing planar bilayer membrane with different phospholipids at a weight ratio of 1 sterol/2 phospholipid. (Erg-C16 tail PC) AmB was added to the *cis*-chamber with ergosterol–DPhPC membrane (molar ratio of 2.52/2.36) at a final concentration of 0.0025 μg/ml. Amplitude histogram of one-sided AmB channel conductance was defined under the same conditions; (Erg-C17 tail PC) AmB was added to the *cis*-chamber with ergosterol-1,2-diheptadecanoyl-*sn*-glycero-3-phosphocholine membrane (molar ratio of 2.52/2.62) at a final concentration of 0.0025 μg/ml; (Erg-egg PC) AmB was added to the *cis*-chamber with ergosterol–egg PC membrane (molar ratio of 2.52/2.60) at a final concentration of 0.0010 μg/ml; (Erg-C18 tail PC) AmB was added to the *cis*-chamber with ergosterol–DOPC membrane (molar ratio of 2.52/2.54) at a final concentration of 0.00025 μg/ml. The membrane separated solution contained 2 M KCl, 10 mM Tris–HCl (pH 7.4). The single-channel records were made at a potential of 115 mV after continuous monitoring of transmembrane current for 15–20 min. *Solid lines* represent zero current

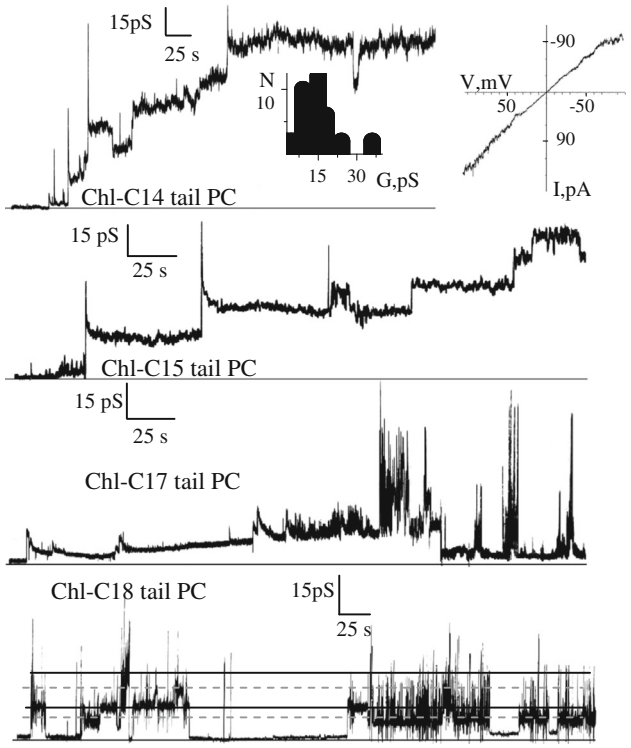

Fig. 3 Single channels created after the addition of AmB from the *cis*-side of cholesterol-containing planar bilayer membrane with different phospholipids at a weight ratio of 1 sterol/2 phospholipid. (Chl-C14 tail PC) AmB was added to the *cis*-chamber with cholesterol–DMPC membrane (molar ratio of 2.59/2.94) at a final concentration of 0.005 μg/ml. Amplitude histogram of one-sided AmB channel conductance and steady-state current–voltage relationship of macroscopic AmB-created current was obtained under the same conditions; (Chl-C15 tail PC) AmB was added to the *cis*-chamber with cholesterol-1,2-dipentadecanoyl-*sn*-glycero-3-phosphocholine membrane (molar ratio of 2.59/2.84) at a final concentration of 0.005 μg/ml; (Chl-C17 tail PC) AmB was added to the *cis*-chamber with cholesterol-1,2-diheptadecanoyl-*sn*-glycero-3-phosphocholine membrane (molar ratio of 2.59/2.62) at a final concentration of 0.005 μg/ml; (Chl-C18 tail PC) AmB was added to the *cis*-chamber with cholesterol–DOPC membrane (molar ratio of 2.59/2.54) at a final concentration of 0.005 μg/ml; the membrane separated solution contained 2 M KCl, 10 mM Tris–HCl (pH 7.4). The single-channel record was made after continuous monitoring of transmembrane current for 15–20-min time at a potential of 115 mV. Stationary current–voltage relationships were measured by the application of a voltage-ramp protocol (−100 to +100 mV, 3.3 min) onto a steady-state macroscopic current achieved on a multitude of channels reconstituted at long monitoring (another 15–20 min) after 15–20-min time limit set for single-channel formation. Channel openings are shown as upward deflections. *Solid lines* represent zero current and the level of open channel discrete conductance. *Dashed lines* represent the substates of discrete channel conductance

cholesterol-containing liposomes (2–5 μg/ml; Romero et al. 2009; Ramos et al. 1989) or native membranes (1.6–5.5 μg/ml; Legrand et al. 1997; Brajtburg et al. 1984).

The single-channel events on solvent-containing BLMs were observed at 10–15 min after addition of AmB at a concentration of 0.0010–0.0025 μg/ml into the solution with 2 M KCl on the *cis*-side of ergosterol–C16 or C17 tail phospholipid membrane and on the *cis*-side of cholesterol–C14–C18 tail phospholipid membranes at AmB concentration of 0.005 μg/ml (Figs. 1a, 2, 3). The separate one-sided AmB channels insertion occurred readily at 10–15 min after addition of AmB at a concentration of 0.00025 μg/ml into the solution with 2 M KCl on the *cis*-side of ergosterol–C18 tail DOPC BLM, while the insertion rate of one-sided AmB channels on the same side of ergosterol–egg PC BLM containing C16 and C18 tails was

random (Fig. 2). The macroscopic current obtained after the insertion of a multitude of one-sided AmB channels in ergosterol–DOPC membrane was at least 50 times higher than the current AmB created on one side of cholesterol–DOPC membrane.

One-sided AmB channels created a conductance peak at 15 pS in all cholesterol–phospholipid membranes and 6–7.5 pS in all ergosterol–phospholipid membranes on the amplitude histograms defined at a membrane potential of 115 mV (Figs. 1a, 2, 3). After the reconstruction on one side of cholesterol–C14–C16 acyl chain phospholipid membranes and ergosterol–C14–C18 acyl chain phospholipid membranes, AmB channels remained mostly open despite the overall decrease in channels life time observed on ergosterol-containing BLMs with C-18 acyl chain phospholipids (egg PC; DOPC; DSPC; Figs. 1a, 2, 3). The most dramatic decrease in one-sided AmB channel open time and conductance occurred on cholesterol-containing BLMs with C-17–C-18 acyl chain phospholipids (1,2-diheptadecanoyl-*sn*-glycero-3-phosphocholine; 1,2-distearoyl-*sn*-glycero-3-phosphocholine; DOPC; Fig. 3). The results obtained on solvent-containing membranes are quite different from those obtained on thin membranes, where under similar conditions Brutyan and McPhie (1996) failed to find the difference between gating of one-sided AmB channels in cholesterol-containing BLM with C16 acyl chain DPhPC and C18 acyl chain DOPC. Though huge diversion between channel open times, it is quite obvious that the most of AmB-induced current decreased on thicker "painted" cholesterol-containing BLMs due to slow separate channel conductance decay better seen on BLM containing C17 acyl chain phospholipid and decrease in channel life time that led to fast degrading of separate channel conductance to substates and long-lasting full closures (see Fig. 3 for current traces on cholesterol–C17 and C18 tail phospholipid bilayers).

It is evident for the creation of the same AmB oligomeric structure that the most probable conductance (11 and 15 pS) established for one-sided AmB channels on thin cholesterol–DPhPC and ergosterol–DphPC bilayers (Brutyan and McPhie 1996) was almost identical with what we found under the same conditions on solvent-containing cholesterol—all tail length phospholipid BLMs (Figs. 1a, 3). Slightly lower conductance of 11 pS determined for AmB channels on solvent-free cholesterol–DPhPC BLM can be attributed to channel's inability to reach the discrete conductance due to its short lifetime reported in Brutyan and McPhie (1996). The overall decrease in most probable one-sided AmB channel conductance we observed on ergosterol-containing BLMs with different tail length phospholipids (7.5 pS for C-16 chain DPhPC; 6 pS for C-17 chain 1,2-diheptadecanoyl-*sn*-glycero-3-phosphocholine; 6 pS for C-18 chain DSPC; 6 pS for C-18 chain DOPC or egg PC) may indicate more frequent assembly of another smaller size oligomer in addition to the already established most common structure (Fig. 2a). This observation proves earlier suggestions made about dependence of AmB–sterol stoichiometry and thus the size of AmB pore on the type of sterol present in the membrane at the aqueous channel formation (Brutyan and McPhie 1996; Romero et al. 2009; Matsumori et al. 2009).

The addition of AmB to both sides of solvent-containing cholesterol–DPhPC and cholesterol–egg PC membrane resulted in appearance of single-channel events with comparable long lifetime but much smaller conductance peak of 1.8 pS at 115 mV voltage applied (Fig. 1b). There seem to be no major discrepancies between our results and earlier reported data on conductance of AmB double-channels defined on solvent-containing (3.9 pS) and thin (4 pS) cholesterol–phospholipid BLMs washed in 2 M KCl containing solution as those were measured at the higher potential of 150 mV (Brutyan and McPhie 1996; Borisova et al. 1979).

In our experiments, separate double-channels of AmB were formed at a drug concentration of 0.0005 μg/ml on each side of membrane, which was tenfold less than critical threshold achieved at one-sided AmB channel formation on cholesterol–DPhPC membrane within 20-min time interval.

It should be noted that 5-min preincubation of AmB in the chamber with cholesterol- and ergosterol-containing phospholipid BLMs followed by continuous stirring at no potential applied greatly facilitated further ionic channels formation for one- and two-sided AmB actions (Figs. 1, 2, 3).

The relative permeability ratio (P^{+}_{Na}/P^{-}_{Cl}) estimated from the shift of the reversal potential according to Goldman–Hodgkin–Katz equation was 6.92 ± 0.48 for steady-state AmB current created on one side of the bilayer membrane (Fig. 4), while (P^{-}_{Cl}/P^{+}_{K}) for double-pores consisted of 5.0 ± 0.31 (Fig. 1b). This coincides favorably with preferential though not ideal cation selectivity of one-sided AmB channels and anion selectivity of AmB double-channels shown before on cholesterol-containing phospholipid membranes (Brutyan and McPhie 1996; Romero et al. 2009; Ostroumova et al. 2012; Ermishkin et al. 1977).

The current–voltage relationship (*I*/*V*) of one-sided AmB channels and AmB double-channels steady-state current was determined by the application of voltage ramp with a protocol (−100 to +100 mV, 3.3 min). Incorporation of AmB from the both sides of cholesterol–DPhPC and cholesterol–egg PC membrane induced a membrane current with superlinear voltage dependence (Figs. 1b, curve 1, 8c, curve 1) similar to those found for AmB double-channel in cholesterol–phospholipid BLMs (Ostroumova et al. 2012; Borisova et al. 1979; Ermishkin et al. 1977).

AmB separately applied to the *cis*-side of cholesterol- and ergosterol-containing membranes induced a steady-state

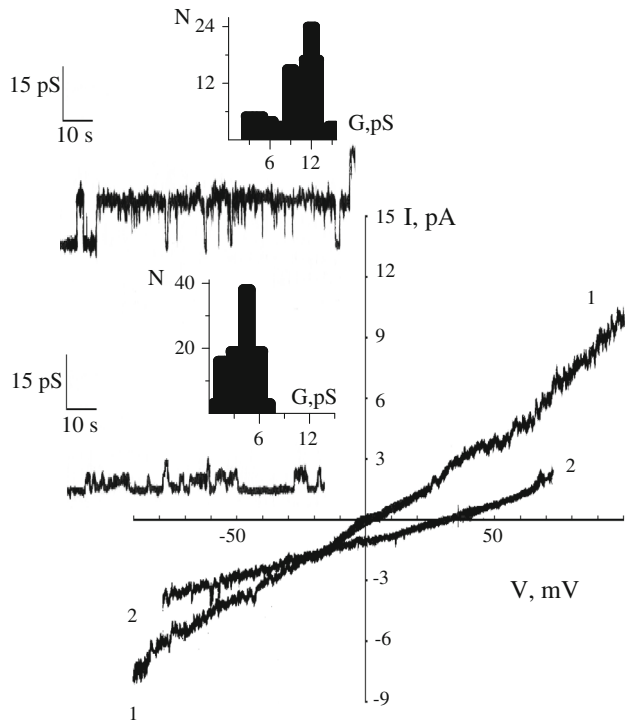

Fig. 4 Steady-state current–voltage relationships and single-AmB channel recordings obtained on cholesterol–DPhPC membrane modified with AmB on the *cis*-side of membrane. *I/V* plots represent steady-state current–voltage relationships of cholesterol–DPhPC membrane (the molar ratio of 2.59/2.36) modified with AmB introduced to the cis-chamber at a final concentration of 0.005 μg/ml. The steady-state macroscopic current AmB created in the symmetrical solution of 2 M NaCl, 10 mM Tris–HCl (pH 7.4; *curve 1*) was achieved due to a current rise occurred after monitoring single-channel events for ~30 min. The macroscopic AmB current was again plotted versus voltage after flushing *cis*-chamber with 80 ml of 0.2 M NaCl, 10 mM Tris–HCl (pH 7.4; *curve 2*). Current traces of one-sided AmB channels were recorded in the symmetrical solutions of 2 M NaCl, 10 mM Tris–HCl (pH 7.4) and 2 M $CaCl_2$, 10 mM Tris–HCl (pH 7.4) at 115 mV voltage applied. Amplitude histograms were created on ~100 separate channel events. The surface of actual bilayer membrane formed on 0.5-mm-diameter hole in Teflon cup was 0.55–0.98 × 10^{-4} cm^2

current that showed slight voltage-dependent rectification in all the salt solutions tested ($CaCl_2$, NaCl, CsCl, LiCl, 2 M; KCl, 0.1 or 2 M) for the phospholipids of all tail lengths. The rectification was weak, passing ~1.4 times more current at +100 mV than at −100 mV (Figs. 3, 4 (curve 1), 8b (curve 1)). The steady-state macroscopic current induced by one-sided AmB channels at +100 and −100 mV on solvent-free cholesterol–PC, cholesterol–DPhPC, ergosterol–PC and ergosterol–DPhPC BLMs depends on the sign of the membrane potential with almost the same rectification (asymmetry coefficient) of ~1.5 (Brutyan and McPhie 1996; Kleinberg and Finkelstein 1984). All above references underline that the increase in AmB-created current at the positive potential on drug addition side of cholesterol- and ergosterol-containing phospholipid membranes corresponds to the physiological situation, where AmB is applied from extracellular side. Therefore, AmB channel in short C14–C16 chains phospholipid environment of plasma membrane could be dangerous for mammalian cells due to its long lifetime and the influence of membrane potential.

The Dielectric Thickness of Solvent-Containing Cholesterol–DPhPC and Cholesterol–PC BLMs

Specific capacitances of cholesterol–DPhPC BLM and cholesterol–egg PC BLM measured by the application of triangular pulse consisted of 0.40 and 0.36 μF/cm^2, correspondingly. Assuming that dielectric constant (ε) is 2.1 for the membrane hydrocarbon region (Montal and Mueller 1972), the respective dielectric thickness (*d*) of cholesterol–DPhPC BLM and cholesterol–egg PC BLM calculated from their specific capacitance was 46.1 and 51.2 Å. Thus, the difference of dielectric thickness for these membranes was 5.1 Å.

The Permeability of AmB Channels Formed on One Side of Solvent-Containing Cholesterol–DPhPC Membrane

The ionic selectivity of one-sided AmB channels was defined by single-channel recordings made after addition of AmB to the *cis*-side of cholesterol–DPhPC BLM in 2 M solutions of different salts. The channels obtained in the solution containing 2 M NaCl had one major conductive state interrupted with short switches to different substates and the closed state, while in 2 M $CaCl_2$, AmB channels exhibited slight conductance changes in the open state followed by much longer closures (Fig. 4). Estimates of AmB channel conductance in 2 M solutions of NaCl, $CaCl_2$, KCl, CsCl and LiCl at membrane potential of 115 mV suggested maximal conductance of 12 pS; 4.5 pS; 15 pS; 16.8 pS; and 4.5 pS, respectively (records in CsCl and LiCl solutions are not shown). Thus, in chloride solutions of univalent cations, channel conductance decreases in the order CsCl > KCl > NaCl > LiCl. Taking into account 6.92-fold increase in permeability of AmB channel for Na^+ versus Cl^- (Fig. 4, curves 1 and 2), we conclude that AmB-induced current is comprised mainly of monovalent cations with a weak preference for K^+ against Na^+. The selectivity of one-sided AmB channel obtained on solvent-containing cholesterol–DPhPC BLM was the same with that of one-sided AmB channel measured on thin cholesterol- and ergosterol–DPhPC or DOPC membranes (Brutyan and McPhie 1996). Hence, the lipid composition and overall membrane thickness are unlikely to influence the ionic permeability of AmB channel formed on one side of lipid bilayer.

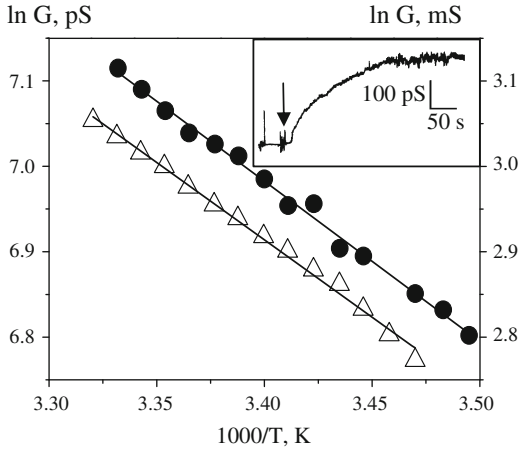

Fig. 5 Typical temperature relationships of steady-state macroscopic conductance AmB induced from the *cis*-side of cholesterol–DPhPC membrane and the conductance of membrane-free saline. The membrane washing solution contained 100 mM KCl buffered in 10 mM Tris–HCl (pH 7.4). The conductance was continuously monitored at a membrane potential of 50 mV. Amphotericin B was applied to the *cis*-side of the membrane at a final concentration of 0.005 μg/ml. *Open triangle symbol* Control experiments carried out in the solution of 100 mM KCl, 10 mM Tris–HCl (pH 7.4) without membrane, *filled circle symbol* steady-state macroscopic conductance AmB created on the cis-side of bilayer membrane. Deviations of mean values do not exceed the size of experimental points. The *left scale* and *filled circles* correspond to AmB-modified membrane, while the *right scale* and *open triangles* represent data obtained in membrane-free bathing solution. The *inset* shows the increase in transmembrane current achieved almost instantly after the application of AmB into near membrane area at a membrane potential of 80 mV. *Arrow* represents the stirring that followed the addition of AmB

Table 1 The one-sided AmB channel conductance and fillings with different nonelectrolytes obtained after reconstitution in cholesterol–DPhPC bilayer membrane

Nonelectrolyte	r_h (Å)	g_i (pS)	χ (mS/cm)	F_i
1. ———		15 ± 0.50	238.0	
2. Ethylene glycol	2.62	6.0 ± 0.25	135.5	1.97
3. Glycerol	3.08	6.75 ± 0.34	130.8	1.49
4. Ribose	3.50	8.25 ± 0.28	130.8	1.00
5. Glucose	3.70	11.3 ± 0.50	129.6	0.39
6. Sucrose	4.67	15 ± 0.43	133.3	0
7. PEG-300	6.00	16.5 ± 0.35	118.3	−0.1
8. PEG-400	7.00	16.5 ± 0.5	127.6	−0.1

All the nonelectrolytes were used at a concentration of 20 % in the membrane bathing fluid containing 2 M KCl and 10 mM Tris–HCl (pH 7.4). r_h are the hydrodynamic radii of NEs as defined in Krasilnikov et al. (1998). The one-sided AmB single-channel conductance was defined from the peak of the amplitude histograms, each obtained on ~100 separate channels (Figs. 1a, 6). The AmB single-channel conductance represents the mean value ± standard errors obtained from unitary channel conductance defined in the histograms; g_i refers to the single-channel conductance determined in the presence of the same nonelectrolyte on both sides of the bilayer membrane; χ is the specific conductivity of the solutions with and without nonelectrolytes; F_i is the ion channel filling calculated by the formalism of Krasilnikov et al. (1998): $F_i = [(g_0 - g_i)/g_i]/[(\chi_0 - \chi_i)/\chi_i]$, where g_0 is the single-channel conductance in the solution without nonelectrolyte, χ_0 is the conductivity of nonelectrolyte-free saline, and χ_i is the conductivity of the saline containing 20 % (w/v) of a given nonelectrolyte. Other conditions are as described in the legends of Figs. 1a and 5

The relative passage rates of alkaline ions through one-sided AmB channels are the same by the disposition in the Eizenman ranges with the order of their mobility in water (Hille 1992). This suggests that water molecules within one-sided AmB channel retain their bulk water properties to a substantial degree, freely entering and leaving the channel. Varying the temperature in the range of 13–28 °C did not affect the resting conductance of unmodified BLM. However, the conductance of one-sided AmB channels was increased by elevating temperature. Conversely, the decreasing temperature reduced the AmB channel conductance. The temperature-induced AmB channels conductance changes calculated at steady temperatures were consistent with those found by the application of temperature ramp. The activation energy measured for steady-state macroscopic current AmB created on the *cis*-side of solvent-containing cholesterol–DPhPC membrane in the solution of 100 mM KCl consisted of 3.6 ± 0.5 kcal/mol (Fig. 5). The activation energy of membrane-free solution with 100 mM KCl was the same (3.61 ± 0.1 kcal/mol) (Fig. 5).

As described by Krasilnikov et al. (1998; Holz and Finkelstein 1970), the addition of nonelectrolytes with different hydrodynamic radii into the membrane bathing solution lowers the conductance of AmB channel when the value of hydrodynamic radius of the nonelectrolyte approaches that of the channel radius. The radii of the channel pores AmB formed on the *cis*-side of solvent-containing cholesterol–DPhPC membrane were defined by the determination of the channel filling (F%) with different nonelectrolyte molecules through both entrances to the channel (Krasilnikov et al. 1998). Assuming that the effective (inner) radius of one-sided AmB channel on the *cis*-side is close to the minimum size of an impermeable nonelectrolyte molecule, the radius of the channel was determined within the transition zone from limited permeation of glucose to impermeability at zero filling of the channel cavity ($F\% = 0$; Table 1; Fig. 6). Thus defined, the radius of one-sided AmB channel was 4.5 Å (Fig. 6). The radius estimated in the presence of the same nonelectrolyte on both sides of the bilayer coincides with the radius of the larger entrance to the channel (Krasilnikov et al. 1998; Shatursky et al. 2007).

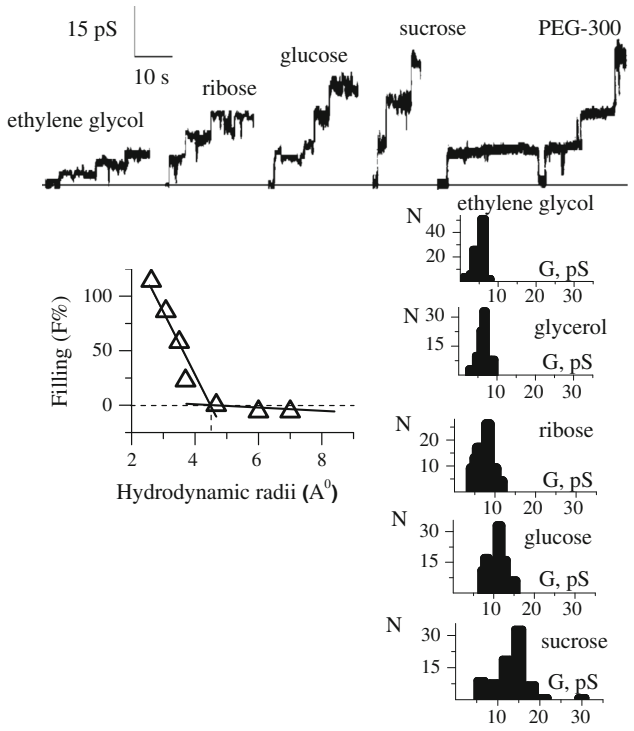

Fig. 6 Dependence of one-sided AmB channel filling from both entrances (F%) on the hydrodynamic radii of nonelectrolytes. In all the experiments, AmB was added to the *cis*-chamber of cholesterol–DPhPC membrane at a final concentration of 0.005 μg/ml. The ion channel filling (F%) was calculated as proposed by Krasilnikov et al. (1998): $F\% = 2F_i/(F_1 + F_2) * 100$ %, where F_i is the filling in the solutions of nonelectrolyte tested; F_1 and F_2 are the fillings in the saline with ethylene glycol and glycerol, respectively. The membrane washing solutions contained 20 % of each nonelectrolyte in 2 M KCl, 10 mM Tris–HCl (pH 7.4). The voltage of 115 mV was applied on the side of drug addition. Single-channel recordings under corresponding conditions are shown on top. Channel openings are upward deflections. *Solid line* represents zero current. The most probable single-channel conductance (see Table 1) was defined from the peaks of the histograms, each obtained on ~100 separate events (shown on the *right side*) in solutions of the same nonelectrolytes from both sides of cholesterol–DPhPC BLM. The conductance of one-sided AmB channels is not shown for glycerol and PEG-400. The pore size was calculated from the intercept of *dashed lines* indicating zero filling with nonelectrolyte molecules. All *solid lines* are best least square fits to the experimental points *triangle symbol*. Standard deviations of each mean value are represented in Table 1. Additional information on experimental conditions is described in Table 1

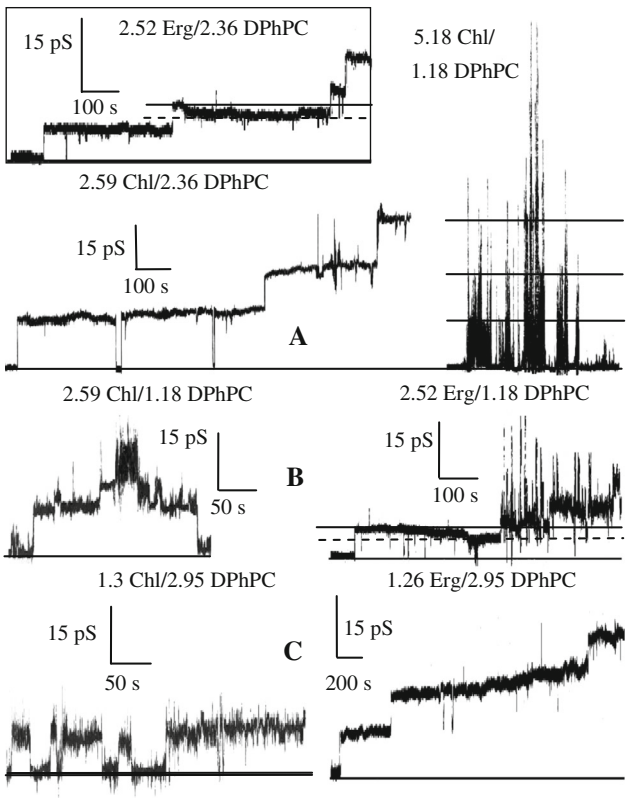

Fig. 7 Dependence of the one-sided AmB channels insertion rate and lifetime on the molar ratio of cholesterol– and ergosterol/DPhPC (Chl/DPhPC and Erg/DPhPC) in bilayer membranes. The cholesterol– and ergosterol/DPhPC molar ratios are represented for separate experiment carried out on a new membrane. The AmB insertion into a membrane formed at a molar ratio of: **a** (*left*) 2.59 Chl/2.36 DPhPC (weight ratio of 1 Chl/2 DPhPC); (*inset*) 2.52 Erg/2.36 DPhPC (weight ratio of 1 Erg/2 DPhPC); (*right*) 5.18 Chl/1.18 DPhPC (weight ratio of 2 Chl/1 DPhPC). **b** (*left*) 2.59 Chl/1.18 DPhPC; (*right*) 2.52 Erg/1.18 DPhPC. The weight ratio of both *left* and *right* cases consists of 1 sterol/1 DPhPC. **c** (*left*) 1.3 Chl/2.95 DPhPC; (*right*) 1.26 Erg/2.95 DPhPC. The weight ratio of membrane lipids was 0.5 sterol/2.5 DPhPC. In all the experiments, AmB was applied from the *cis*-side of membrane at a final concentration of 0.005 μg/ml. The saline contained 2 M KCl, 10 mM Tris–HCl (pH 7.4). Single-channel recordings were made after continuous monitoring of transmembrane current for 15–20 min at a potential of 115 mV. Channel openings are shown as upward deflections. *Solid lines* represent zero current and the discrete conductance of open channel. *Black dashed lines* represent the substates of discrete channel conductance. The surface of actual bilayer membranes formed on 0.5-mm-diameter hole in Teflon cup was 0.55–0.98 × 10^{-4} cm^2

The Influence of the Type of Membrane Sterol and its Concentration on One-Sided AmB Channel Formation and Functioning

The change in cholesterol/DPhPC molar ratio in BLM had no influence on the conductance of one-sided AmB channels. Instead, it affected the insertion rate and channels lifetime as it took place at the change in lipid composition (Figs. 2, 3, 7). The replacement of cholesterol with ergosterol increased the amount of smaller conductance one-sided AmB channels (6–7 pS) and changed the channels lifetime at different ergosterol/DPhPC molar ratios (Figs. 2, 7).

The AmB channels incorporated on the *cis*-side of BLM formed of cholesterol– or ergosterol–DPhPC mixture at a molar ratio of ~1 (weight ratio 1 sterol/2 DPhPC) exhibited long lasting minutes openings interrupted by both long (up to 10 s) and rare short (≤1 s) closures (Fig. 7a). The approximate rate of insertion into this BLM consisted of 1

channel over 4-min time for both sterols. The increase in cholesterol/DPhPC or ergosterol/DPhPC molar ratio decreased the lifetime of one-sided AmB channels in solvent-containing bilayers dramatically since sterol/DPhPC molar ratio rose from 1 to 2 (weight ratio of 1 sterol/1 DPhPC; Fig. 7b). The long openings decreased, while some of the channels exhibited short-duration current bursts (each opening lasted seconds and less) that looked similar to the observations made by Brutyan and McPhie (Brutyan and McPhie 1996) on thin cholesterol-containing DOPC or DPhPC BLMs at the longest time scale. Meanwhile, at above condition (weight ratio of 1 sterol/1 DPhPC), the rate of AmB channels incorporation into solvent-containing BLM had developed to 1 channel per 2.5 min (Fig. 7b). Further increase in cholesterol/DPhPC molar ratio of solvent-containing BLM to 5 (weight ratio of 2 cholesterol/1 DPhPC; Fig. 7a, right) left primarily short-duration current bursts without long-lasting openings. Assuming that the separate AmB channel conductance was 15 pS, the rate of channel insertion rose further to ~1 channel per 20 s. The one-sided AmB channel lifetime now resembles current records had been made on thin cholesterol–DPhPC membrane (Brutyan and McPhie 1996) although Brutyan and McPhie (1996) used cholesterol–DPhPC BLM at a molar ratio of ~0.5. Thus, despite similar results on AmB membrane action obtained by the use of thin (Brutyan and McPhie 1996; Kleinberg and Finkelstein 1984) and solvent-containing ergosterol– and cholesterol–phospholipid membranes within the whole range of phospholipids tested, the lifetime of one-sided AmB channel is inadequately shorter on solvent-free cholesterol–DPhPC BLM as compared with that on solvent-containing cholesterol–DPhPC BLM (Figs. 2, 3, 7a). This is proved by the creation of channels with long open states on the *cis*-side of solvent-containing cholesterol– and ergosterol–DPhPC BLM at the same with Brutyan and McPhie (1996) molar ratio of ~0.5 (weight ratio of 0.5 sterol/2.5 DPhPC; Fig. 7c). In this case, the decrease in cholesterol/DPhPC molar ratio led to a significant reduction in AmB channels insertion rate to 1 channel per >10 min time.

The Blocking Effects of DMHT, TEA and TMA Determined on AmB-Modified Solvent-Containing Cholesterol–DPhPC, Cholesterol–Egg PC and Ergosterol–DPhPC Planar Lipid Bilayers

Introduction of DMHT (0.1 mM) to the *cis*-side of cholesterol–DPhPC BLM washed in symmetrical solution containing 100 mM KCl reduced steady-state macroscopic current AmB created from the same side of membrane by 84 ± 2 % at the membrane potential of 50 mV (Fig. 8a, curves 1 and 2). The DMHT-induced block of

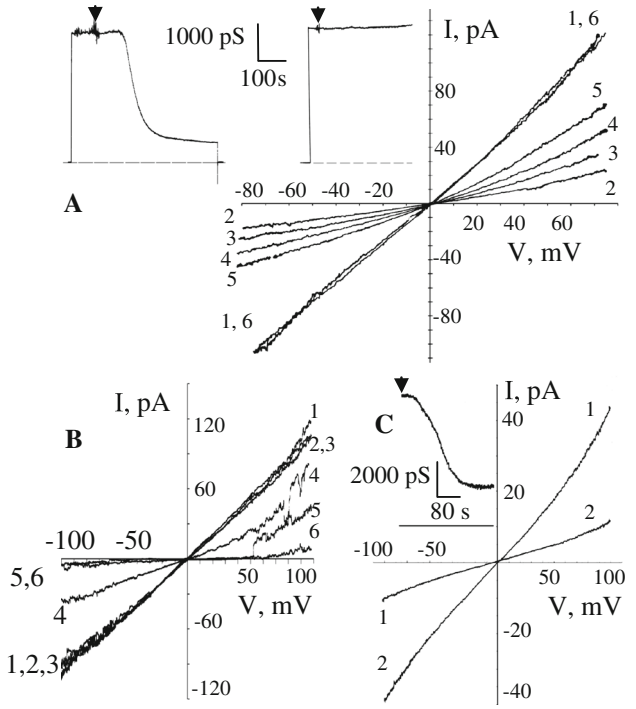

Fig. 8 Blocking of steady-state macroscopic current of AmB-created one-sided channels and double-channels in sterol–phospholipid membranes by DMHT (0.1 mM). *Arrows* indicate the addition of DMHT. **a** Current–voltage relationships of one-sided AmB channels in cholesterol–DPhPC membrane elicited using the voltage-ramp protocol (−80 to +80 mV, 2.64 min): *1*—in DMHT-free saline; *2*—8 min after addition of DMHT to the *cis*-side of membrane; *3,4,5,6*—next 2, 5, 11 and 12 min (30-min overall) past after a flashing of *cis*-compartment with DMHT-free saline. The *inset* represents: (*left*) the time trace of AmB-induced current at 50 mV after addition of DMHT to the *cis*-side; (*right*) the time trace of AmB-induced current at 50 mV after addition of DMHT to the *trans*-side. *Dashed lines* show zero current. The cholesterol–DPhPC membrane was bathed in the solution of 100 mM KCl, 10 mM Tris–HCl (pH 7.4). Macroscopic currents were achieved after near membrane application of AmB (0.02 μg/ml) on the *cis*-side. **b** Current–voltage relationships of macroscopic steady-state current of one-sided AmB channels reconstituted from the *cis*-side of ergosterol–DPhPC membrane. The final concentration of AmB on the *cis*-side was 0.005 μg/ml. The current–voltage dependences obtained by the application of voltage-ramp protocol (−100 to +100 mV, 3.3 min): *1*—in DMHT-free solution of 2 M KCl, 10 mM Tris–HCl (pH 7.4); *2,3*—4 and 8 min after addition of DMHT (0.1 mM) to the *trans*-side, correspondingly; *4,5,6*—2.5, 5 and 7.5 min after addition of DMHT to the *cis*-side, correspondingly. **c** Current–voltage relationships of AmB double-channels in cholesterol–egg PC membrane obtained by the application of voltage-ramp protocol (−80 to +80 mV, 2.64 min): *1*—in DMHT-free solution of 2 M KCl, 10 mM Tris–HCl (pH 7.4); *2*—8 min after addition of DMHT to the *cis*-side. The *inset* represents time trace of AmB-induced current in the solution of 100 mM KCl, Tris–HCl (pH 7.4) at 50 mV voltage after addition of DMHT to the *cis*-side. *Solid line* shows zero current. Macroscopic currents were achieved at a final AmB concentration of 0.005 μg/ml on both sides of membrane

transmembrane current across one-sided AmB channels fully developed over 7–8 min (Fig. 8a, inset) exhibiting no significant dependence on the sign of membrane potential

within the range of voltages clamped (Fig. 8a, curves 1 and 2).

DMHT effectively blocked macroscopic current through one-sided AmB channels on one side of membrane only, while the portion of these channels located on the opposite side of membrane remained unaffected as the addition of DMHT (0.1 mM) to the *trans*-side of membrane did not change the membrane conductance (Fig. 8a, inset). DMHT (0.1 mM) also caused similar one-sided reduction in the steady-state macroscopic current through AmB-created current in ergosterol–DPhPC membrane (Fig. 8b, curves 1–3 and curves 3–6) and quasi-steady-state (slowly decreasing) macroscopic current of AmB-modified cholesterol–egg PC membrane (data not shown). This is very consistent with earlier reports on the asymmetrical blocking action of TEA defined for one-sided AmB channels (Brutyan and McPhie 1996). The DMHT block of one-sided AmB channels achieved from the *cis*-side of membrane was reversible. A thorough flushing of *cis*-compartment with 80 ml of membrane bathing saline that did not contain DMHT completely restored the conductance of AmB channels within 25–30 min (Fig. 8a, curves 1–6).

The addition of DMHT (0.1 mM) to the *cis*-side of cholesterol–DPhPC and cholesterol–egg PC BLMs blocked macroscopic current induced by AmB double-channels in solutions containing 100 mM KCl and 2 M KCl by 70 ± 3.5 % (Fig. 8c). The DMHT-induced block of transmembrane current across AmB double-channels fully developed over 7–8 min (Fig. 8c, inset) without significant dependence on the sign of membrane potential clamped (Fig. 8c, curves 1 and 2).

Testing the effectiveness of 0.1 mM DMHT on the *cis*-side of single-AmB channels formed from the same side of cholesterol–DPhPC membrane revealed 78.5 ± 1.5 % blocking in the solution with 2 M KCl at a potential of 115 mV. As shown in Fig. 9a, left DMHT block developed through three phases within 40–45-s time. At first, DMHT caused small increase in current seen straight after the DMHT addition than, at second phase, the current gradually decreased until the step-like closure of AmB channel occurred at the last phase. The current at this completely closed state was different from zero and interrupted by occasional short (<1 s) openings that could not reach the discrete level at the resolution time set for the record. Hence, DMHT blocks one-sided AmB channel by reducing its current and lifetime. Addition of DMHT to the *trans*-side of membrane did not change the conductance of AmB channel formed on the opposite side of membrane (see Fig. 9a, right). This confirms the asymmetrical action of DMHT on macroscopic and single-channel currents AmB created from one side of the membrane. The DMHT block achieved from the *cis*-side of AmB double-channels proves Brutyan's and McPhie (1996) suggestion that one-sided

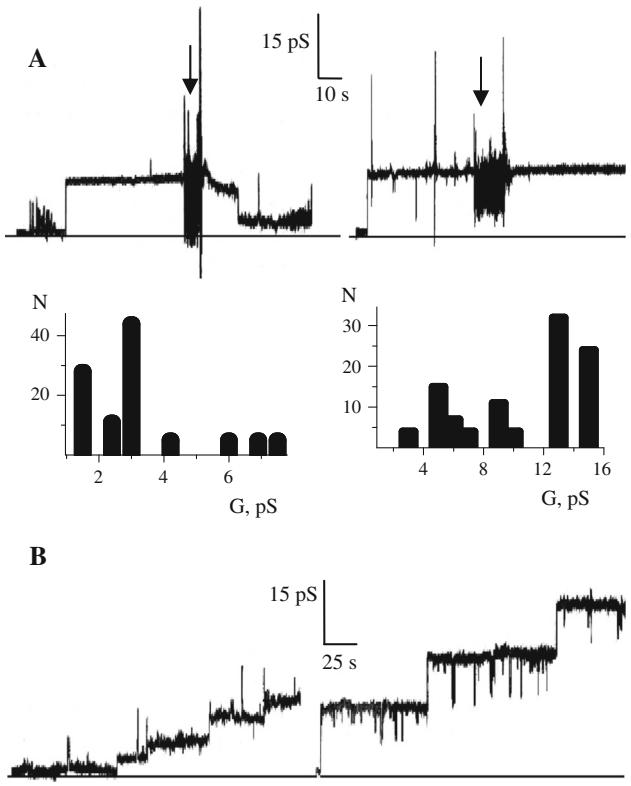

Fig. 9 DMHT block of single-AmB channels formed from the *cis*-side of cholesterol–DPhPC membrane. Amphotericin B was added to the *cis*-chamber at a concentration of 0.005 mg/ml. The membrane washing solution contained 2 M KCl, 10 mM Tris–HCl (pH 7.4). The holding potential was 115 mV. **a** *Left side* The 0.1 mM DMHT concentration was applied from the side of drug addition onto a current induced by single AmB channel. *Right side* The DMHT at a concentration of 0.1 m M was applied onto a current induced by single AmB channel oppositely to the side of drug addition (from the *trans*-side). *Arrows* indicate the addition of DMHT under continuous stirring. **b** (*top*) Amplitude histograms of AmB channels formed in the presence of 0.1 mM DMHT on the side the AmB was introduced to (shown on the *left*) and on the opposite side of membrane (shown on the *right*). (*Bottom*) Single-AmB channels formed in the presence of 0.1 mM DMHT on the side of drug addition (on the *left* side) and on the opposite side of membrane (on the *right* side). In all experiments, channel openings are upward deflections and *solid lines* represent zero current. The surface bilayer membrane occupied within dimension of Teflon cup aperture was $\sim 0.55 \times 10^{-4}$ cm^2

channels have nonidentical entrances on the opposite sides of membrane, where only *cis*-entrance is identical with both entrances to the symmetrical channel.

The one-sided AmB channel formation was also recorded in the presence of 0.1 mM DMHT on the different sides of BLM as the blocker was added before AmB (Fig. 9b). In this case, AmB channels created on the *cis*-side of membrane showed small stationary level conductance with a peak at 3 pS (see amplitude histogram in Fig. 9b, left) interrupted by short (lasting seconds and less) openings, when DMHT was on the side of drug addition (Fig. 9b, *bottom*, left). Assuming that the one-sided AmB

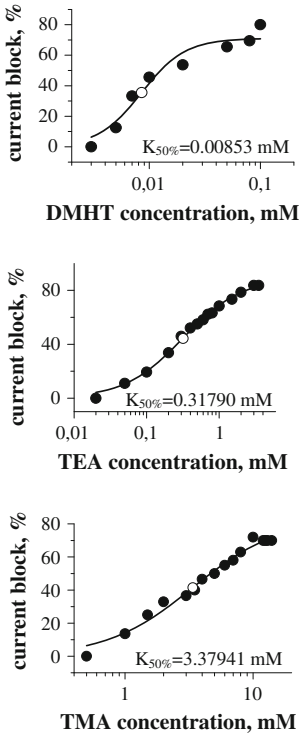

Fig. 10 Macroscopic current induced by one-sided AmB channels in the cholesterol–DPhPC membrane against different concentrations of DMHT, TEA and TMA applied from the side of AmB addition. The membrane separated fluid consisted of 100 mM KCl, 10 mM Tris–HCl (pH 7.4) and blockers at concentrations indicated on *horizontal* log scales. Transmembrane current was continuously monitored at 50 mV voltage-clamp conditions. Each *black circle* on the *panel* represents the consecutive concentration of blocker. The blocking percentages indicated (*vertical scales*) are those achieved at the steady state. The plots are best sigmoidal growth fits to the experimental points. Each *panel* shows the dependence of transmembrane current created by one-sided AmB channels upon different concentrations of DMHT (*Top*), TEA (*Middle*) and TMA (*Bottom*). A half of maximum binding rate represented on each *panel* and the slopes (see "Results") were calculated in Hill coordinates. The AmB was added to the *cis*-side of cholesterol–DPhPC membrane at a final concentration of 0.03–0.07 μg/ml

channel formation was also followed by short (lasting seconds and less) current jumps (Fig. 1a, left), the increases in transmembrane current on left panel of Fig. 9b (*bottom*) are most likely to result from the insertion of DMHT-blocked AmB channels. This suggestion is proved by the increase in channel conductance peak to 13 pS when AmB channels were reconstituted in the presence of DMHT on the *trans*-side of membrane (Fig. 9b, *bottom*, right) that almost restored 15 pS conductance measured for one-sided AmB channels without blocker (Figs. 1a, right, 9b, right). The difference in peak conductance (3 and 13 pS) defined for one-sided AmB channels indicates that *cis*-addition of 0.1 mM DMHT prior to channel formation on the same side of membrane blocked ~80 % of AmB-induced current in 2 M KCl at 115 mV potential with no apparent change in blocked channel lifetime. Thus, DMHT (0.1 mM) causes similar asymmetrical block of AmB-induced macroscopic current and single-channel events on the side of channel formation.

The DMHT block of macroscopic current AmB induced on the *cis*-side of BLM washed in the solution containing 100 mM KCl has shown slight S-like dependency upon the concentration of blocker applied. The reduction in AmB-induced current occurred steeply in an exponential manner with increasing DMHT concentrations and reached saturation approximately at 0.02 mM (Fig. 10, *top*). A half of maximum binding velocity was reached at a DMHT concentration of 8.53 μM. The DMHT dissociation constant (K_d) determined in Hill coordinates was $10^{-5.07}$ M with the slope of 2.2, suggesting the involvement of several AmB or DMHT sites in binding.

The solvent-containing cholesterol–DPhPC membranes modified by the multitude of AmB channels on the *cis*-side were also titrated with different concentrations of well-known blockers, TEA and TMA in order to compare their actions with that of DMHT. Addition of TEA (3 mM) or TMA (10 mM) to the *cis*-side of AmB-modified bilayer membrane bathed in solution containing symmetrical 100 mM KCl blocked macroscopic current across one-sided AmB channels by 81.6 ± 5 and 70 ± 4 %, respectively (Fig. 10, *middle, bottom*). The TEA- and TMA-induced reduction in current through one-sided AmB channels depended on the TEA and TMA concentrations and could be described by a saturation curve (Fig. 10). The AmB-created current change also occurred quite steeply and reached its saturation approximately at 0.75 mM of TEA and at 4 mM of TMA. One half of maximum binding speed with one-sided AmB channels was achieved at TEA concentration of 0.32 mM and at TMA concentration of 3.38 mM. The TEA and TMA K_ds determined in Hill coordinates were $10^{-3.5}$ and $10^{-2.47}$ M with the slopes of 1.08 and 1.29, respectively. The lack in positive cooperativity found for both tetraalkylammonia suggests their primary binding to only one site of the one-sided AmB channel. The binding of one-sided AmB channel with all the blockers tested took place on the same side of the channel as none of the blockers changed AmB-induced current when applied from the opposite side of the membrane. All the blockers, including DMHT, caused similar reduction in quasi-steady-state macroscopic current created on the cis-side of solvent-containing cholesterol–egg PC BLM.

Discussion

The membranes of cholesterol–DPhPC and cholesterol–egg PC were used for dielectric thickness measurements

because, according to our results (Figs. 1a, 2, 3) the difference between their hydrocarbon interiors lined with 3,7,11,15-tetramethylhexadecanoic acid residues of DPhPC and oleic acid residues of egg PC is likely to determine the changes in lifetime for one-sided AmB channel. Furthermore, the solvent-containing BLMs formed from phospholipids and cholesterol at a weight ratio of 2:1 are well known as uncharged and stable (Fajkus and Hianik 2002). Even though cholesterol–DPhPC membrane thickness can hardly be regarded as a major limitation for one-sided AmB action, the estimates of the difference between capacitance of cholesterol–DPhPC BLM and cholesterol–egg PC BLM could shed the light on local thinning of lipid bilayer around one-sided AmB channel. Although due to a limited oil or water penetration the dielectric thickness of solvent-containing and solvent-free BLMs is expected to be smaller than the actual thickness of BLMs and native membranes (Montal and Mueller 1972; Gross et al. 2011), this does not affect the mean value of the difference between the thicknesses of similar type of membranes (solvent-containing bilayers) with different lipid composition. Hence, the difference of dielectric thickness between cholesterol–DPhPC BLM and cholesterol–egg PC BLM (5.1 Å) is quite similar with the length of two carbon and one hydrogen bonds (4.17 Å) that makes egg PC molecule with 18 carbons tail longer than 16 carbons tail DPhPC molecule. Obtained results prove the formation of a stable ion-conducting AmB channel on one side of solvent-containing bilayer formed from cholesterol and phospholipid, which longest acyl chain is only 4–5 Å shorter than the most common 18 carbons acyl chain of egg PC molecule.

Brutyan and McPhie (1996) noted tenfold decrease in one-sided AmB channel lifetime in solvent-free ergosterol–C18 tail DOPC BLM with overall dielectric thickness of 25.1 Å that in our case of much thicker solvent-containing cholesterol–egg PC membrane (51.2 Å) resulted in gradual macroscopic current decay back to zero level because the acyl chain of 9-*cis*-octadecanoic fatty acid residue of DOPC has the same amount of carbons with oleic acid residue of egg PC. It should be noted that the difference in dielectric thickness of solvent-free ergosterol–DOPC and ergosterol–DPhPC membranes (Brutyan and McPhie 1996) was though smaller (~2 Å) but still comparable with the difference between dielectric thickness of solvent-containing cholesterol–egg PC and cholesterol–DPhPC membranes (5.1 Å). Assuming that 2–5 Å change in membrane thickness at DPhPC replacement with DOPC in thin ergosterol-containing membrane caused tenfold reduction in channels lifetime to 1.3 s (Brutyan and McPhie 1996) and the transition from long open states (minutes) on solvent-containing cholesterol–DPhPC (Fig. 1a) to very brief channel openings lasting only fractions of a second on solvent-containing cholesterol–egg PC BLM (data not shown; see Fig. 3 for comparable C18 chain DOPC), the expected difference in length between extended DOPC/egg PC and DPhPC molecules (4.17 Å) appears to be the main factor one-sided AmB channel lifetime depends on. The actual change in membrane thickness necessary for the above AmB channel lifetime transition on solvent-containing membrane is even closer to that of solvent-free membrane (~2 Å) as the short openings first appeared on solvent-containing cholesterol–C17 tail phospholipid BLM (Fig. 3). This suggests the reduction of 5.1 Å difference in dielectric thickness between solvent-containing cholesterol–DPhPC and cholesterol–egg PC membranes at least by the length of one carbon bond (~1.54 Å) to 3.56 Å.

The results of the investigations of one-sided AmB action on solvent-containing and thin (Brutyan and McPhie 1996) BLMs formed from cholesterol and DPhPC (Fig. 1a) suggest that AmB-created single-channel events can be observed at much lower concentrations (0.005–0.018 μg/ml) than those required for BLMs or liposomes formed from cholesterol and native phospholipids (2–10 μg/ml; Marty and Finkelstein 1975; Romero et al. 2009). Even lower concentrations than critical threshold stated here (0.005 μg/ml) could still produce single-AmB channels on one side of 46.1 Å solvent-containing cholesterol–DPhPC BLM when membrane current was monitored for more than 20 min time limit at the membrane potential of 115 mV. This again coincides with the conclusion about potential dependency of one-sided AmB channel formation in thin BLMs (Brutyan and McPhie 1996), where applied potential could increase the AmB concentration on the membrane surface or force yet nonaqueous AmB channel inside the membrane since the increase in near membrane AmB concentration has resulted in formation of pre-pore aggregate. The formation of one-sided AmB channel can also be greatly facilitated by drug preincubation at zero membrane potential as shown in solvent-containing cholesterol–DPhPC membrane. In this case, the adsorption of AmB monomers on membrane can be initiated by hydrophobic interaction between heptane side of AmB macrolide ring and membrane phospholipid hydrocarbon chains as the surface of solvent-containing BLM made of cholesterol and DPhPC at a weight ratio of 1:2 is thought to be uncharged (Fajkus and Hianik 2002). This favors intramembrane option proposed by Brutyan and McPhie (1996) where polyene side of lactone ring partitions into the extracellular layer of membrane to establish hydrophobic bonds with the acyl chains of phospholipid molecules. Moreover, while the membrane cholesterol is known to induce partial insertion of AmB monomers into membrane due to disordering the surface of lipid bilayer, the ergosterol exhibited even more disordered state of phospholipid membrane at the level of hydrocarbon chains and in the mobility of the choline headgroups (Urbina et al. 1995).

Resulting alternation in more and less tightly packed lipid leads to creation of "wells" appropriate for vertical or angled insertion of the pore-forming monomers and their consecutive aggregation into a channel pre-pore on membrane surface (Rossjohn et al. 1997; Shepard et al. 2000; Flanagan et al. 2009). Then, 7.2-fold decrease in AmB concentration threshold necessary for single-channel formation on solvent-containing cholesterol–phospholipid BLMs (0.005 μg/ml) and ~10-fold decrease in AmB concentration (0.001–0.0025 μg/ml) on solvent-containing ergosterol–phospholipid BLMs (except for DOPC) versus AmB concentration threshold obtained on thin cholesterol– and ergosterol–phospholipid membrane (0.036 and 0.018 μg/ml, correspondingly; Brutyan and McPhie 1996) can be explained by increased ability of almost twice thicker heptane-containing membrane to accommodate AmB monomers oriented most appropriately for the formation of ion-conducting oligomer. Perhaps, the greater ability of thicker solvent-containing BLMs to accept the fraction of vertically oriented or angled AmB monomers (Gagos′ et al. 2005) allows to skip (at least partially) the stage of transition from horizontal adhering of amphiphilic AmB monomers to planar membrane to the formation of V-shaped AmB oligomer (Cohen 2010). Additional sevenfold increase in one-sided AmB channel formation on solvent-containing ergosterol–DOPC or ergosterol–egg PC BLMs (threshold AmB concentration of 0.00025 μg/ml) as compared to that observed on solvent-containing ergosterol-saturated chains phospholipid BLMs was a likely result of lipid bilayer disordering by unsaturated chains of 9-*cis*-octadecanoic fatty acid of DOPC or most common oleic and linoleic acids of egg PC (Urbina et al. 1995).

It should be noted that AmB was capable of forming one-sided channels with similar pore size or stoichiometry, asymmetry of *I*/*V* relationships, ionic selectivity and asymmetrical blocking by TEA, TMA and DMHT in all types of solvent-containing and thin sterol–phospholipid bilayers (Brutyan and McPhie 1996), thereby suggesting the resemblance of ion-conductive oligomers.

The coincidence of the activation energy measured for AmB channels in the solution of 100 mM KCl (3.6 ± 0.5 kcal/mol) and the activation energy of membrane-free solution with 100 mM KCl (3.61 ± 0.1 kcal/mol) proves that the entrance to one-sided AmB channel is large enough to admit an easy access and exit of water molecules. The same mobility of alkaline ions in this channel and bulk water results from lining the channel interior with large amount of water molecules. According to different computer simulations, this amount varies from 25 to more than 75 water molecules inside AmB channel (10 Å diameter) formed in cholesterol-containing membrane (Baginski et al. 1997; Khutorsky 1996). Thus, any molecule of appropriate size passing through this pore significantly interacts with water. Slightly enlarged mouth of the one-sided AmB channel is formed on the extracellular side due to intermolecular hydrogen bonds between amino group of lactol ring at C_{19} carbon of major lactone ring of AmB molecule and the carboxyl group at C_{16} carbon of the adjacent AmB molecule. These bonds form a stable hydrogen bond ring that determines the size of channel entrance on the side of drug addition to the target cell or BLM (Marty and Finkelstein 1975; Baginski et al. 1997). The size of one-sided AmB channel mouth determined on solvent-containing cholesterol–DPhPC BLM (4.5 Å) is similar with AmB water pore dimension that admits the permeation of glucose with Stokes radius of 4.2 Å (Tejuca et al. 2001) and completely hydrated Ca^{2+} (Cohen 2010). Interestingly, that the latest computer simulations based on concerted intermolecular =C–H···O interactions between AmB monomers suggested that one-sided AmB channel with almost the same inner radius of 4.4 Å can be created by a hexamer (Lisnyak 2012) instead of conventional deca- or octamer (Marty and Finkelstein 1975; Baginski et al. 1997).

Two- to fourfold decrease in AmB concentrations observed at separate channel formation on solvent-containing ergosterol–C16–C17 saturated chain phospholipids and large 20-fold fall of AmB concentration (seen occasionally with egg PC and readily repeatable in the presence of DOPC) in comparison with channel formation on solvent-containing cholesterol–phospholipid membranes (Figs. 1a, 2, 3) prove the ergosterol-dependent increase in AmB toxicity on fungi (Cohen 2010; Bolard et al. 1991; Brutyan and McPhie 1996). The fact that the macroscopic current induced by one-sided AmB channels in solvent-containing ergosterol–DOPC membrane was 50 times higher than AmB-created current across solvent-containing cholesterol–DOPC membrane is also in agreement with the increase in one-sided AmB channel forming ability on thin ergosterol– versus cholesterol–phospholipid membranes (Cohen 2010; Brutyan and McPhie 1996). Even the lifetime of one-sided AmB channels in both solvent-containing and thin cholesterol–phospholipid BLMs decreases to the fractions of a second in the presence of phospholipids with C18 acyl chain while retaining long open states that last tens of seconds in ergosterol-containing BLMs.

The data on molecular structure and membrane action of one-sided AmB channels in solvent-containing BLMs are consistent with the AmB–sterol channel model proposed by the classic and most of resent research (Cohen 2010). The sterol requirement and the number of carbons in phospholipid acyl chains ranging from 16 to 18 (Kleinberg and Finkelstein 1984) are the major influence on lifetime of one-sided AmB channel (Figs. 2, 3, 7). Thus, the main discrepancy between one-sided AmB channels created in solvent-containing and thin bilayer membranes consists in different open channel

lifetimes on solvent-containing and thin cholesterol–C16 tail DPhPC membrane (Brutyan and McPhie 1996). The duration of one-sided AmB channel lifetime in solvent-containing and thin sterol–C16 tail DPhPC BLMs and sterol–C16, C18 tails egg PC or C18 tail DOPC BLMs can be determined by the similar difference of dielectric thickness (~2–5 Å) between solvent-containing or thin sterol–C18 tail and sterol–C16 tail phospholipid membranes. This suggests that the overall size of solvent-containing BLM hydrocarbon core does not prevent C14–C16 tail phospholipid molecules from thinning around AmB molecule to the extent where local membrane thickness is approximately equal to the length of one-sided channel.

In classical models of aqueous AmB channel, the stability and thus long lifetime of AmB channel formed on the *cis*-side of solvent-containing and solvent-free BLMs can be explained by the preferential hydrogen bonding between hydroxyls at C_{35} carbons of lactone ring immersed into lipid bilayer (tail part of the channel) and polar heads of phospholipid from the *trans*-side of membrane (head-to-tail mode). Therefore, the drastic decrease in one-sided AmB channel lifetime rather depends on the compatibility of the difference between dielectric thickness of sterol-containing C16 and C18 tail phospholipid bilayers (~2–5 Å) and the size of one-sided AmB channel constriction inside lipid bilayer with the apparent radius just barely smaller than that of the channel mouth (~3.7 Å; Fig. 6; Shatursky et al. 2009). Thus, the polar heads of adjacent to one-sided AmB channel phospholipids with C14–C16 acyl chains have enough space within *trans*-side leaflet of bilayer to swing towards the channel tail and on the channel tail itself to create hydrogen bonds that effectively lock ion-conductive channel inside solvent-containing cholesterol–C14–C16 tails phospholipid membrane for the time of long channel opening (Fig. 3). The increased amount of failures by longer acyl chains of synthetic 1,2-diheptadecanoyl-*sn*-glycero-3-phosphocholine, DOPC and egg PC to establish above head-to-tail connection ends up in a mode, where preference is given to hydrogen bonding between hydroxyls positioned at C_{35} lactone ring carbons and hydrocarbon tails of phospholipid molecules located on the *trans*-side of BLM (tail-to-tail mode). Tail-to-tail mode is likely to result in quasi-steady-state of macroscopic currents achieved after one-sided AmB application to the near membrane area of solvent-containing cholesterol–egg PC BLM, similar decay of microscopic current across separate one-sided AmB channels shown in solvent-containing cholesterol–C17 tail phospholipid BLM (Fig. 3) and the decrease in one-sided AmB channel lifetime observed on solvent-containing cholesterol–C17–C18 tail phospholipid BLMs (Fig. 3), solvent-containing ergosterol–C18 tail phospholipid BLM (Fig. 2), thin ergosterol–C18 tail phospholipid BLM and thin cholesterol–C16,C18 tail phospholipid BLMs (Brutyan and McPhie 1996). It is possible that Brutyan and McPhie (1996) did not distinguish between decrease in channel lifetime powered by the change in membrane thickness on thin cholesterol–C16 and C18 phospholipid bilayers because of cholesterol-driven "condensing effect" (Cohen 2010). The "condensing" of thin, free of solvent BLMs could be more efficient than that of solvent-containing BLMs packing much tighter membrane forming molecules (including cholesterol) around one-sided AmB channel that better screened charged groups on the channel tail within thin bilayers. This suggestion seems particularly evident since ergosterol lacks in ability to produce similar "condensing effect" with PC and DOPC due to their unsaturated chain (Cohen 2010; Urbina et al. 1995). Hence, some polar heads of adjacent to one-sided AmB channel phospholipids with C18 acyl chain (DOPC and egg PC) that still are capable of making head-to-tail connections yet have enough space to swing to the channel tail and create hydrogen bonds. These bonds keep one-sided AmB channel inside solvent-containing and thin ergosterol–C18 tail phospholipid BLMs for tens of seconds (Fig. 2; Brutyan and McPhie 1996), while highly ordered thin cholesterol-containing DPhPC and DOPC membranes let one-sided AmB channel inside membrane for less than 1-s time (Brutyan and McPhie 1996). It is, therefore, possible that less ordered structure of solvent-containing bilayer allowed to distinguish the difference between open times of one-sided AmB channel on cholesterol-containing membranes with C16 and C18 acyl chain phospholipids (Fig. 3). The same fast gating of one-sided AmB channels in thin (Brutyan and McPhie 1996) and solvent-containing cholesterol–DPhPC BLMs at ~10 times higher cholesterol/DPhPC molar ratio of the solvent-containing bilayer (Fig. 7a, right) provides additional evidence in favor of less screening of the channel tail by phospholipid and cholesterol within solvent-containing membranes.

The AmB–sterol interaction is supposed to be another factor facilitating one-sided channel formation as direct participation of sterol molecules in the structure of one-sided AmB water pore may substitute head-to-tail connections with hydrophobic bonds between adjacent cholesterol and phospholipid tails (Cohen 2010). The AmB–sterol interaction may also cause the AmB monomers to target rich in cholesterol lipid rafts of mammalian cells creating microdomains where AmB water pores are preferentially formed (Romero et al. 2009). Considering similar though reduced for ergosterol, ability of both sterols in ordering phospholipid bilayers (Coutinho et al. 2004) and the fact that reach in ergosterol lipid rafts were also found in fungi (Hsueh et al. 2005), the same molecular events can be anticipated upon creation of one-sided AmB channels in ergosterol-containing membranes. The formation of one-sided AmB channels in solvent-containing bilayer membranes indicates that AmB

water pores are capable of increasing the transmembrane current of cations (K^+, Na^+, Ca^{2+}) across some of plasma membrane lipid raft area besides lipid bilayer of the target cell plasma membrane. This proves the earlier assumptions that one-sided AmB channels can be preferentially localized at the boundary of raft and nonraft bilayer of the target cell because the thickness of bilayers at the membrane center of the sterol-enriched rafts is greater than that of nonraft bilayers (Gandhavadi et al. 2002).

The cholesterol/phospholipid molar ratio appreciably greater than ~ 1 takes place in mammalian cell plasma membrane when the cell is at a pathological state. This ratio increases up to 1.3–1.6 in cholesterol-fed animals and patients with liver disease, while normally in plasma membranes of rat liver cells, it consists of 0.58, only (Collins and Phillips 1982). Despite some controversy (Hsueh et al. 2005), the ergosterol/phospholipid molar ratio determined in plasma membranes of different fungi also does not exceed the value of ~ 1. Moreover, assuming that the ergosterol/phospholipid molar ratio found for *Leishmania promastigotes* was 0.32 (Ramos et al. 1990) and 0.46 for *Saccharomyces cerevisiae* (Hsueh et al. 2005), it is possible to point out the obvious similarity of these ratios with the cholesterol/phospholipid molar ratios obtained on plasma membranes of higher eukaryotic cells (Schneiter et al. 1999). Therefore, faster gating of one-sided AmB channels observed on solvent-containing BLMs at the abnormal cholesterol– and ergosterol/phospholipid molar ratio of ~ 2 (Fig. 7b) was likely to result from enhanced screening of the charged channel tail by membrane components due to sterol-induced ordering of phospholipid bilayer (Coutinho et al. 2004) and increased amount of membrane sterols.

Most of long open AmB channels appeared in heptane-containing BLM since its cholesterol– and ergosterol/phospholipid molar ratio has become ~ 1 (Fig. 7a, left). Further decrease in cholesterol– and ergosterol/phospholipid molar ratio in solvent-containing BLMs to 0.44 (Fig. 7c) did not affect the longevity of channel open state while reducing the amount of channels in the membrane. This leads to believe that AmB channel in ergosterol–C16–C18 tail phospholipid membrane and cholesterol–C14–C16 tail phospholipid membranes mostly exists at the open state, considering that cholesterol– and ergosterol/phospholipid molar ratios 0.44–1 are those that occur in plasma membrane under normal conditions (Figs. 2, 3, 7a, left, c).

It should be noted that one-sided AmB channel is also capable locally of increasing cholesterol concentration in the membrane by removing cholesterol molecules from interactions with phospholipid (Cohen 2010). Therefore, we cannot fully exclude the possibility that sufficient decrease in AmB channel lifetime observed on thick solvent-containing BLM at higher molar ratio 5.18 cholesterol/1.18 DPhPC (Fig. 7a, right) than that of thin BLM (2.59 cholesterol/5.9 DPhPC; Brutyan and McPhie 1996) may result from slower increase in local cholesterol concentration around the channel within thick bilayer (Baginski et al. 1997). Hence, despite much lower overall cholesterol concentration in thin membrane (2.59 mol cholesterol/5.9 mol DPhPC), its concentration around one-sided AmB channel complies with that of reach in cholesterol solvent-containing membrane causing similar reduction in channel lifetime.

Alternatively, AmB could fail to form long open one-sided ion-conductive channel in thin cholesterol–phospholipid BLM due to cholesterol-induced high orderly state of its surface ("condensing effect"; Nagle et al. 2008) that allowed to lying on the membrane AmB pre-pore aggregate only short time-to-time penetrations of membrane core as suggested by Brutyan and McPhie (1996). Than, long open one-sided AmB channels Brutyan and McPhie (1996) observed on thin ergosterol–phospholipid BLM could appear as a result of more disordered state ergosterol caused at the level of membrane hydrocarbon chains and increased mobility of the choline headgroups as compared with cholesterol-containing membrane (Urbina et al. 1995). This can facilitate AmB pre-pore penetration into thin ergosterol-containing BLM and further creation of long open one-sided AmB channel, possibly, by establishing hydrogen connections between molecules of AmB and phospholipid in head-to-tail mode (Marty and Finkelstein 1975; Brutyan and McPhie 1996). Thus, the reduction in channel long lifetime less obvious versus cholesterol-containing bilayers but still observed in solvent-containing ergosterol–C18 tail phospholipid membrane (Fig. 2) can be explained, primarily, by decreased ability of longer acyl chain phospholipid to bind charged tail of the channel.

The data obtained on solvent-containing cholesterol–phospholipid membranes strongly suggest that deepened into membrane AmB pre-pore can stay inside becoming a long open ion-conducting water pore in the surrounding of 14–16 carbon chains phospholipid. This occurs due to membrane thinning mechanisms that regulate ion channel function of amphiphilic drug by local adjustment of the bilayer thickness in order to match the channel length (Lundbæk 2008; Marty and Finkelstein 1975; Brutyan and McPhie 1996). In mammalian cells, this can be achieved on rich in sphingomyelin exoplasmic leaflet of human erythrocytes, particularly as C16 acyl chain hexadecanoyl sphingomyelin is one of the predominant species around AmB channel at the boundary of raft and nonraft bilayer. The C14 acyl chain myristic acid can also be involved as it has sufficiently high hydrophobicity to become incorporated into the fatty acyl core of the eukaryotic cell plasma membrane. Long open ion-conducting AmB channel may

appear even within predominantly C18 chain native PC or sphingomyelin, when surrounded by the tails of palmitic acid residue or sphingosine part of octadecanoyl sphingomyelin ceramide core, correspondingly.

The formation of almost indefinitely open one-sided AmB channels in sterol–short-chain phospholipid surrounding of target cells causes efflux of K^+ and influx of extracellular Na^+ resulting in cell shrinkage or swelling. Instead of a cell death, the irregular ionic distribution is more likely to make the AmB-treated cell to waist its resources to recover the loss of intracellular K^+ or unnecessary gain of Na^+ or Ca^{2+} (Yano et al. 2009). This particularly harms already weaken patients as ion regulatory mechanisms in mammalian cells are capable of preventing the lethal effects of AmB water pores for longer periods than fungi (Walev and Bhakdi 1996). Therefore, further development and application of novel AmB sensitive blockers in addition to already existing drug delivery formulations may improve the situation where high AmB toxicity nearly negated its use to the limits of most life-threatening systemic fungal infections (Hartsel and Bolard 1996; Glasser and Murray 2011).

We have shown that a relatively novel thiazole derivative, DMHT also proven to inhibit nystatin channels (Shatursky et al. 2010), effectively blocked AmB channels (Figs. 9, 10). Since none of the cork blockers (TEA and TMA) or DMHT added to the *trans*-side of the solvent-containing and thin BLMs (Brutyan and McPhie 1996) never changed transmembrane current via AmB channels reconstituted on the *cis*-side of membrane, the comparative analysis of their blocking capabilities was available on one side of membrane only. According to classical model of one-sided AmB channel, the sum of electrostatic potential at the channel mouth is negative that could provide a reasonable explanation of asymmetrical noncooperative binding with TEA^+ and TMA^+. Slight positive cooperativity of binding kinetics found for $DMHT^+$ may appear due to additional hydrophobic interaction with a long-chain hydrocarbon tail at position 3 of thiazole moiety as positively charged nitrogen within thiazole cycle binds to oppositely charged channel entrance (Shatursky et al. 2007). Although the overall reduction in AmB-created transmembrane current by DMHT, TEA and TMA is rather similar and falls within the ranges between 70 and 80 %, binding with the DMHT exhibited much higher affinity ($pK = 5.07$; Fig. 10).

Thus, the ability of thiazole and ammonium derivatives to block one-sided AmB channel may occur by the charged end of the blockers passing down the oppositely charged channel mouth and binding there, while their hydrocarbon tails insinuate themselves into the hydrophobic region of the channel walls, and therefore, the space available to them within the channel is larger than that accessible for ions of regular saline bathing the membrane. The intensity of transmembrane current reduction increases with increasing coincidence between the hydrodynamic radius of the blockers and the inner radius of the pore entrance (4.5 Å). Hence, DMHT blocks one-sided AmB channel by entering the channel mouth and locking it (Fig. 9a, left). Insufficient temporary increase in one-sided AmB channel conductance observed instantly at the introduction of DMHT into membrane separated saline can happen due to increased mobility of K^+ in the membrane bathing solution caused by impermeable DMHT molecules. The increased mobility of K^+ in the solutions containing DMHT results in larger concentration of potassium ions inside the one-sided AmB channel as compared with the regular amount of K^+ within the channel in symmetrical solution of DMHT-free saline. This mechanism is also held responsible for the slight increase in single-channel conductance observed in the solutions with impermeable PEG-300 and PEG-400 (Table 1; Fig. 6; Shatursky et al. 2007; Krasilnikov et al. 1998). Unlike impermeable nonelectrolytes, DMHT induces only temporary increase in AmB-created current until entering the channel mouth where current starts to decrease in exponential decay mode. Gradual current decrease turns into a momentary step-like channel closure as the blocker reaches fully locked position within the channel mouth. The data on cork-like blocker properties of DMHT are consistent with the decrease in DMHT blocking ability achieved on smaller size mouth of nystatin channel (Shatursky et al. 2010).

However, the blocking mechanism discussed for almost permanently open one-sided AmB channel is not explanatory for double-channel as none of cation blockers should be able to enter its positively charged middle part. It is possible that this potential is only appreciable in the middle part of the AmB double-channel thus preventing cations from passing through, unless they partner up with anions as electro-neutral ion pair (Borisova et al. 1986; Khutorsky 1996). Meanwhile, the channel entrance retains its predominantly negative charge induced by hydroxyls of lactone ring as the channel mouth stays in polar environment. This increases the facilitating role of positive potential applied on the side of membrane the blocker was added to as in double-channel mode the tail part of former one-sided channel is not in contact with water or heads of the lipid molecules. The lack of polar environment in the middle of AmB double-pore also reduces efficacy of $DMHT^+$ block (Fig. 8c) and causes less specific TEA^+ to leave the channel at negative membrane potentials (Borisova et al. 1979).

Conclusion

The reduction in one-sided AmB channel lifetime obtained in solvent-containing cholesterol–phospholipid membranes

with increasing length of phospholipid tails from 16 to 18 carbons underlies the key role of the difference in length between 16 and 18 carbon tails of membrane PC in the regulation of AmB channel toxicity on mammalian cells. The formation of long open one-sided AmB channels in solvent-containing cholesterol–C14–C16 tail phospholipid bilayers and ergosterol–C16–C18 tail phospholipid bilayers suggests that the AmB channel cytotoxicity on plasma membrane of mammalian cell can be similar with that on fungi within the environment of 14–16 carbon lipid chains. The one-sided AmB channel formation and lifetime within the surrounding of 16 carbon acyl chains depends primarily on the amount of membrane sterol as different concentrations of membrane cholesterol and ergosterol caused similar changes in the channel insertion rate and lifetime. Assuming that within the phospholipids of native membrane, 16 carbon tails are almost as often as 18 carbon tails further administration of AmB for clinical use may have to be reconsidered. It is possible that the application of novel AmB channel blockers like DMHT compound may help reduce high AmB toxicity.

Acknowledgments The authors are greatly indebted to Dr. E.V. Grishin of Shemyakin and Ovchinnikov Institute of Bioorganic Chemistry, Russian Academy of Sciences, Moscow, Russian Federation, and Dr. M.D. Kursky of Palladin Institute of Biochemistry, Ukrainian National Academy of Sciences, Kiev, Ukraine, for all kinds of advice and support that helped us to find the leads to this project. We also appreciate the suggestions and criticism of Dr. R.K. Tweten of The University of Oklahoma College of Medicine. Special thanks to Drs V.S. Telezhkin of Cardiff University and University College London, Cardiff & London, UK, P. Yarova of Kings College, London, UK, and M.V. Kustov of Bogomolets Institute of Physiology, Ukrainian National Academy of Sciences, Kiev, Ukraine, for friendly advice and support. This work was funded by the decision of Research Council of Palladin Institute of Biochemistry, Kiev, Ukraine, and Bogomolets National Medical University, Kiev, Ukraine.

References

Baginski M, Resat H, McCammon JA (1997) Molecular properties of amphotericin B membrane channel: a molecular dynamics simulation. Mol Pharmacol 52:560–570

Bernardi P, Rasola A (2007) Calcium and cell death: the mitochondrial connection. Subcell Biochem 45:481–506

Bolard J, Legrand P, Heitz F, Cybulska B (1991) One-sided action of amphotericin B on cholesterol-containing membranes is determined by its self-association in the medium. Biochemistry 30:5707–5715

Borisova MP, Ermishkin LN, Silberstein AYa (1979) Mechanism of blockage of amphotericin B channels in a lipid bilayer. Biochim Biophys Acta 553:450–459

Borisova MP, Brutyan RA, Ermishkin LN (1986) Mechanism of anion-cation selectivity of amphotericin B channels. J Membr Biol 90:13–20

Brajtburg J, Elberg S, Medoff J, Kobayashi GS, Schlessinger D, Medoff G (1984) Stimulatory, permeabilizing, and toxic effects of amphotericin B in L cells. Antimicrob Agents Chemother 26:892–897

Brutyan RA, McPhie P (1996) On the one-sided action of amphotericin B on lipid bilayer membranes. J Gen Physiol 107:69–78

Cohen BE (2010) Amphotericin B membrane action: role for two types of ion channels in eliciting cell survival and lethal effects. J Membr Biol 238:1–20

Collins J, Phillips MC (1982) The stability and structure of cholesterol-rich codispersions of cholesterol and phosphatidylcholine. J Lipid Res 23:291–298

Coutinho A, Silva L, Fedorov A, Prieto M (2004) Cholesterol and ergosterol influence nystatin surface aggregation: relation to pore formation. Biophys J 87:3264–3276

Ermishkin LN, Kasumov KM, Potseluyev VM (1977) Properties of amphotericin B channels in a lipid bilayer. Biochim Biophys Acta 470:357–367

Fajkus M, Hianik T (2002) Peculiarities of the DNA hybridization on the surface of bilayer lipid membranes. Talanta 56:895–903

Flanagan JJ, Tweten RK, Johnson AE, Heuck AP (2009) Cholesterol exposure at the membrane surface is necessary and sufficient to trigger perfringolysin O binding. Biochemistry 48:3977–3987

Gagos′ M, Gabrielska J, Dalla Serra M, Gruszecki WI (2005) Binding of antibiotic amphotericin B to lipid membranes: monomolecular layer technique and linear dichroism- FTIR studies. Mol Membr Biol 2:433–442

Gandhavadi M, Allende D, Vidal A, Simon SA, McIntosh TJ (2002) Structure, composition, and peptide binding properties of detergent soluble bilayers and detergent resistant rafts. Biophys J 82:1469–1482

Glasser J, Murray C (2011) Case report: central nervous system toxicity associated with liposomal amphotericin B therapy for cutaneous leishmaniasis. Am J Trop Med Hyg 84:566–568

Gross LCM, Heron AJ, Baca SC, Wallace MI (2011) Determining membrane capacitance by dynamic control of droplet interface bilayer area. Langmuir 27:14335–14342

Hartsel S, Bolard J (1996) Amphotericin B: new life for an old drug. TiPS 17:445–449

Hille B (1992) Ionic channels in excitable membranes. Sinauer, Sunderland

Holz R, Finkelstein A (1970) The water and nonelectrolyte permeability induced in thin lipid membranes by the polyene antibiotics nystatin and amphotericin B. J Gen Physiol 56:515–526

Hsueh Ya-Wei, Gilbert K, Trandum C, Zuckermann M, Thewalt J (2005) The effect of ergosterol on dipalmitoylphosphatidylcholine bilayers: a deuterium NMR and calorimetric study. Biophys J 88:1799–1808

Khutorsky V (1996) Ion coordination in the amphotericin B channel. Biophys J 71:2984–2995

Kleinberg ME, Finkelstein A (1984) Single-length and double-length channels formed by nystatin in lipid bilayer membranes. J Membr Biol 80:257–269

Krasilnikov OV, DaCruz JB, Yuldasheva LN, Varanda WA, Nogueira RA (1998) A novel approach to study the geometry of the water lumen of ion channels: Colicin Ia channels in planar lipid bilayers. J Membr Biol 161:83–92

Legrand P, Che′ron M, Leroy L, Bolard J (1997) Release of amphotericin B from delivery systems and its action against fungal and mammalian cells. J Drug Target 4:311–319

Lisnyak YuV (2012) Models of amphotericin membrane channel based on concerted =C–H···O intermolecular interactions. Ann Mechnikov Inst 3:33–37

Lundbæk JA (2008) Lipid bilayer-mediated regulation of ion channel function by amphiphilic drugs. J Gen Physiol 131:421–429

Maeng S, Ko YJ, Kim GB, Jung KW, Floyd A, Heitman J, Bahn YS (2010) Comparative transcriptome analysis reveals novel roles of the Ras and cyclic AMP signaling pathways in environmental stress response and antifungal drug sensitivity in Cryptococcus neoformans. Eukaryot Cell 9:360–378

Marty A, Finkelstein A (1975) Pores formed in lipid bilayer membranes by nystatin. J Gen Physiol 65:515–526

Matsumori N, Tahara K, Yamamoto H, Morooka A, Doi M, Oishi T, Murata M (2009) Direct interaction between amphotericin B and ergosterol in lipid bilayers as revealed by 2H NMR spectroscopy. J Am Chem Soc 131:11855–11860

Montal M, Mueller P (1972) Formation of bimolecular membranes from lipid monolayers and study of their electrical properties. Proc Nat Acad Sci USA 69:3561–3566

Mueller P, Rudin DO, Tien HT, Wescott WC (1962) Reconstitution of cell membrane structure in vitro and its transformation into an excitable system. Nature 194:979–980

Nagle JF, Mathai JC, Zeidel ML, Tristram-Nagle S (2008) Theory of passive permeability through lipid bilayers. J Gen Physiol 131:77–85

Ostroumova OS, Efimova SS, Schagina LV (2012) Probing amphotericin B single channel activity by membrane dipole modifiers. PLoS ONE 7:1–6

Ramos HA, de Murciano A, Cohen BE, Bolard J (1989) The polyene antibiotic amphotericin B acts as a Ca^{2+} ionophore across sterol-containing liposomes. Biochim Biophys Acta 982:303–306

Ramos H, Milhaud J, Cohen BE, Bolard J (1990) Enhanced action of amphotericin B on *Leishmania mexicana* resulting from heat transformation. Antimicrob Agents Chemother 34:1584–1589

Romanenko AV, Gnatenko VM, Vladimirova IA, Vovk AI (1995) Pre- and post-synaptic modulation of neuromuscular transmission in smooth muscles by thiazole analogs of vitamin B_1. Neurophysiology 27:297–306

Romero EA, Valdivieso E, Cohen BE (2009) Formation of two different types of ion channels by amphotericin B in human erythrocyte membranes. J Membr Biol 230:69–81

Rossjohn J, Feil SC, McKinstry WJ, Tweten RK, Parker MW (1997) Structure of a cholesterol-binding thiol-activated cytolysin and a model of its membrane form. Cell 89:685–692

Schneiter R, Brügger B, Sandhoff R, Zellnig G, Leber A, Lampl M, Athenstaedt K, Hrastnik C, Eder S, Daum G, Paltauf F, Wieland FT, Kohlwein SD (1999) Electrospray ionization tandem mass spectrometry (ESI–MS/MS) analysis of the lipid molecular species composition of yeast subcellular membranes reveals acyl chain-based sorting/remodelling of distinct molecular species en route to the plasma membrane. J Cell Biol 146:741–754

Shatursky OYa, Volkova TM, Romanenko OV, Himmelreich NH, Grishin EV (2007) Vitamin B_1 thiazole derivative reduces transmembrane current through ionic channels formed by toxins from black widow spider venom and sea anemone in planar phospholipid membranes. Biochim Biophys Acta 1768:207–217

Shatursky OYa, Romanenko OV, Himmelreich NH (2009) Action of vitamin B_1 structural analogue 3-decyloxycarbonylmethyl-4-methyl-5-(β-hydroxyethyl)thiazole chloride on transmembrane current created by ionic channels of amphotericin B in bilayer lipid membrane. Ukr Biochim Zh 81:57–67

Shatursky OYa, Romanenko OV, Himmelreich NH (2010) Effect of 3-decyloxycarbonylmethyl-4-methyl-5-(β-hydroxyethyl)thiazole chloride on nystatin-created K^+-current across bilayer lipid membrane. Ukr Biochim Zh 82:42–51

Shepard LA, Shatursky O, Johnson AE, Tweten RK (2000) The mechanism of pore assembly for a cholesterol-dependent cytolysin: formation of a large prepore complex precedes the insertion of the transmembrane β-hairpins. Biochemistry 39:10284–10293

Tejuca M, Dalla Serra M, Potrich C, Alvarez C, Menestrina G (2001) Sizing the radius of the pore formed in erythrocytes and lipid vesicles by the toxin sticholysin I from the sea anemone Stichodactyla helianthus. J Membr Biol 183:125–135

Urbina JA, Pekerar S, Le HB, Patterson J, Montez B, Oldfield E (1995) Molecular order and dynamics of phosphatidylcholine bilayer membranes in the presence of cholesterol, ergosterol and lanosterol: a comparative study using 2H-, 13C- and 31P-NMR spectroscopy. Biochim Biophys Acta 1238:163–176

Venegas B, Gonza′lez-Damia′n J, Celis H, Ortega-Blake I (2003) Amphotericin B channels in the bacterial membrane: role of sterol and temperature. Biophys J 85:2323–2332

Walev I, Bhakdi S (1996) Possible reason for preferential damage to renal tubular epithelial cells evoked by amphotericin B. Antimicrob Agents Chemother 40:1116–1120

Yano T, Itoh Y, Kawamura E, Maeda A, Egashira N, Nishida M, Kurose H, Oishi R (2009) Amphotericin B-induced renal tubular cell injury is mediated by Na^+ influx through ion- permeable pores and subsequent activation of mitogen-activated protein kinases and elevation of intracellular Ca^{2+} concentration. Antimicrob Agents Chemother 53:1420–1426

Zager RA (2000) Polyene antibiotics: relative degrees of in vitro cytotoxicity and potential effects on tubule phospholipid and ceramide content. Am J Kidney Dis 36:238–249